Author response to the revised manuscript version

June 18, 2021

This document repeats the questions of all referees with the corresponding authors' responses on a point to point basis. Additionally, it indicates for every comment the changes made in the manuscript and explains the reasons of the authors if needed. All page and line references refer to the revised manuscript version. We introduced a numbering of the comments and hope that it reflects the referees view. Appended to this document is a differential view between the first and revised version for convenient tracking of the applied changes.

1 Comments Referee 1

1.1 General Comments

R2: **The authors state at the end of section 4 that the "discrepancy in the [ISRF] values is quite significant" and that "we believe that depending on the mission parameters, this effect should be taken into account for the assessment of the ISRF stability and consequently the performance of the SH". But then in the next sentence they state: "We also conclude, that for the Sentinel-5/UVNS instrument the impact of this effect is of second-order and does not degrade the performance of the SH significantly". This important conclusion is however stated without any further motivation or evidence. It also seems contradictory to the previous sentence. In contrast, the error budget from tables 1 to 3 should be discussed in view of the S5 ISRF requirements error budget, which is intimately linked to the Sentinel-5 product requirements and quality. In this respect, the nature of the S5-ESA scene should be discussed. Is this scene referring to the type 2 non-uniform scene as defined by the S5 system requirements document (Appendix A)? While this is meant to represent a realistic scene with inhomogeneities representing a more averaged land situation, the still moderate and more randomly distributed signal variations result in quite uniform smeared out signal conditions in along-track direction (averaged over the 7km across-track footprint of S5). So the 75% scene presented her seems to be a more realistic case for typical non-uniform scenes, with sharp surface type transitions (city or desert to vegetation, or land to water). The latter seems never to meet the 2% ISRF shape error budget of the S5 SRD not even for a normally distributed PSF.).**

Response: We confirm that the S5-ESA scene is referring to the type 2 non-uniform scene as defined by the S5 SRD. We will describe the derivation of this scene in more detail.
In our manuscript, the calibration scenes refer to conditions with a sudden transition from bright to dark illumination without accounting for motion smear of the satellite platform. These scenes will be used for static on-ground laboratory measurements of the slit homogenizer performance and to validate the prediction models. We agree, that we should make the use case of these scenes more clear and that the ISRF distortions associated with the calibration scenes are not representing real flight measurements but will only be measured in the laboratory. The resulting ISRF errors are exaggerated with respect to real in-flight scenarios. In the revised version of the manuscript we will describe the realistic scenes from the SRD and make our performance assessment based on

these realistic scenes. We will only keep an exemplary 50% stationary calibration scene result and emphasize their use case and the resulting exaggerated ISRF distortions.
The aberrations present in the Sentinel-5/UVNS spectrograph are dependent on the position on the FPA in spectral and spatial direction. Further, the specific aberration type of the final instrument will not be determined but only the RMS spot sizes. In a revised manuscript we will consider several other types of aberration and also their mixing behaviour to make a more thorough and realistic case of the Sentinel-5/UVNS spectrograph.

Changes in manuscript: In section (3), we added a derivation and explanation of the origin of the applicable Earth scene for the Sentinel-5/UVNS mission as defined by ESA in the system requirement document (SRD). We put the calibration scenes into perspective, as they are only used in laboratory measurements. Further, we will mention that measurements over extreme albedo variations are excluded from the Sentinel-5/UVNS mission requirements as stated in the SRD.

R2: **1. I think it would be interesting to also add the expected ISRF error for an optics without SH to the results (tables) presented in Section 4, if that would be possible. Since this would provide the reference with respect to the currently flying push-broom missions.**

Response: We will include simulation results of the case with no slit homogenizer present in order to compare with push-broom missions using a classical slit.

Changes in manuscript: The simulation results for a case of a classical slit are presented in Table (1) and (2). In Figure (7a), we show an ISRF comparison plot with and without SH for a 50 % calibration scene.

R2: **2. The reasoning for making the case for slit-homogenizations, as presented in the context of future missions with even higher spatial resolution like CO2M (Section 3, line 195ff), is a bit confusing. Although I understand, what the authors intend here. The relevance for CO2M is not in terms of CO2 emission inhomogeneities, but again, as for the other missions, in terms of radiances variation. The latter is in the extreme cases governed by clouds and surface and not dominated by atmospheric constituents. Especially the variation of CO2 emission is at times at the sub percent level to the background, therefore not contributing to radiance scene homogeneities. However, underlying variations in surface reflection (e.g. transitions of cities to rural land and lakes) may cause significant ISRF distortions without proper slit-homogenizations, which then, in turn would affect the very high accuracies needed to quantify the elevated CO2 emission plume concentrations. So in this respect NO2 emissions may provide a better example of a single point variations, although even there I would assume that the largest effect on NO2 retrieval accuracies due to ISRF distortions is still originating from surface variations or cloud edges.**

Response: We agree and will revise this section.

Changes in manuscript: The references to the CO2M mission have been removed from the manuscript and we discuss the analysis solely with respect to Sentinel-5/UVNS.

1.2 Editorial comments

R2: **1. Section 1, line 34ff: I would add here the linear detector array spectrometer with scanning mirrors like GOME-1/2 and SCIA have a large IFOV in along-track direction and a box-cart like PSF. You could also mention GOME-2 [Munro et al.,**

2016] in this respect.

Response: We will add this information.

<u>Changes in manuscript:</u> see lines 44-46.

R2: **2. Section 2.1, line 106. Shouldn't this reference be to Fig. 3b and not a?**

Response: Indeed, this will be changed.

<u>Changes in manuscript:</u> see line 122.

R2: **3. Section 2.2, line 128: missing space.**

Response: Done.

<u>Changes in manuscript:</u> see line 149.

2 General comments Referee 2

2.1 General comments/Specific Comments

R2: **0. It is understood that pupil inhomogeneity is introduced by far-field interference originating from wave propagation within the mirror-based SH (creating multiple coherent sources), and would not occur with a classical slit. The far-field non-uniformities are also independent from the achieved near-field homogenisation, and are not a consequence of "remaining" inhomogeneities. This should be stated more clearly in the text (both, if this understanding is correct and if not).**

Response: In general, the near-field and far-field after the SH are correlated by Fourier transform as stated in this paper. But the reasons for the non-uniformity have different origins. The remaining inhomogeneities at the SH exit plane are a result of interference effects of the light propagating through the SH in combination with diffraction. However, the non-uniformity of the pupil illumination originates from the reallocation of the angular distribution of the light exiting the SH in combination with interference effects in the pupil plane. We will state this more clearly in the revised version.

<u>Changes in manuscript:</u> see lines 155-159.

R2: **1. Limitation of the analysis to a single wavelength in a single band, which is insufficient to draw far-reaching conclusions on the performance of wide-bandwidth multiplespectrometer instruments.[...]**
While the methodology and the developed model seem adequate to analyze the impact of using a one-dimensional slit homogeniser, the present analysis is rather limited, and should be extended to come to more meaningful results w.r.t Sentinel-5 and potentially other space missions. The single analysed wavelength is in the NIR band of Sentinel-5, but Fig. 2 shows the SWIR-3 spectrum (with CO, CH_4 and H_2O absorption). The SWIR-3 is likely the most critical band in terms of the impact on retrieved products (e.g. CH_4 and CO column densities). This is due to the deep absorption structures and the relatively high spectral resolution (although the O_2 A-band in the NIR may also be critical). It is therefore recommended to extend the analysis at least to the SWIR-3 band at 2.3 µm (and ideally also SWIR-1 at 1.6µm).

The mathematical model should still be valid for these spectral ranges, and the results would give an impression on the wavelength-dependency of pupil inhomogeneity and its impact on the ISRF. At minimum, please explain why the analysis was not performed for the SWIR-3 band plotted in Fig. 2. In this case it is suggested to replace the plot by the NIR. Another important extension of the analysis would the application to other wavelengths within the chosen band. The main impact of ISRF distortion (or knowledge error) is due to its variation within the spectral band used for the retrieval of the targeted molecular species. The results for one wavelength (or spectral channel) at 760nm reported here give no insight in intra-band variability. However, ISRF knowledge is required over the entire spectral range. Please discuss the expected variation of the results with wavelength. Do they only differ in terms of the contrast, which is lower in deep absorption lines?Do the errors in the figure-of-merit (shape, FWHM, and centroid position) scale linearly with contrast?

Response: We agree, the analysis that we presented only considers a single wavelength point in the NIR channel which contains only limited information about the general SH performance and as pointed out by the referee is also not the most critical one in terms of the retrieved products. However, it is not our intention in this work to provide a full validation of the SH for the Sentinel-5/UVNS missions which will be part of the characterization and calibration campaign. Instead, we wanted to investigate phenomenologically the impact of a non-uniform spectrograph illumination and provide a simulation approach to assess the impact on the ISRF. We therefore propose to present the analysis in the SWIR-3 band instead of the NIR for two reasons. First, as already mentioned this is the more interesting channel in terms of retrieval products. Second, the SH is known to show better performance for smaller wavelengths, as the peak to valley variations in the SH transfer function are stronger for higher wavelengths. This will result in a reduced homogenization performance.
The far field effects that we investigate are driven by geometrical arguments and diffraction, which only vary slightly in a single wavelength channel. Therefore, the expected changes of intraband variability are small. This is particularly the case for the SWIR-3 channel in which the bandwidth is small compared to the wavelength.

Changes in manuscript: The entire manuscript has been adapted to the SWIR-3 wavelength channel.

R2: **2. Limitation to four artificial input scenes, none of which representing a realistic in-flight scenario (even though one is referred to as "representative Earth scene").[...] The S5-ESA-scene used in this study, on which the compliance statement for Sentinel-5 is based on, remains obscure, in the sense that its origins and generation remain unclear. Although it is referred to as "representative Earth scene", the very low contrast plotted in figure 5 does not appear realistic for a ground-scene with considerable contrast. The instrument is likely to frequently see much higher contrast in orbit, e.g. when flying over cloud fields (bright in the NIR) or water bodies (dark in the SWIR). It is suspected that the authors picked one wavelength (in the continuum of the NIR band) of an artificial contrast scene from the S5 requirement documents, and convolved a brightdark step transition with the motion boxcar of the ALT spatial sample (please confirm or not). This is however not flight-representative, as such artificial reference scenes are typically designed to specify straylight performance, not to define a representative geophysical scenario. In order to demonstrate its relevance to expected Sentinel-5 performance, the authors shall clarify the origin and processing of the "S5-ESA-scene". What are the geophysical assumptions behind the scene ? Was it convolved to account for "motion smear" over the ALT spatial sampling distance? It is also recommended to extend the analysis to more than just one (basically flat) convolved transition, in stating compliance of the mission. The method would even allow to explore the maximum contrast transition, which would**

still lead to compliant ISRF knowledge requirements for the Sentinel-5 instrument. This would represent a relevant performance prediction for Sentinel-5, and greatly enhance the scope of the conclusions. The three other scenes considered (25%,50%, and 75% ALT slit illuminated) are also artificial (even impossible to be observed in flight). However they could serve the purpose of highlighting the criticality of pupil inhomogeneity for on-ground calibration. The authors should comment on the implications of their results for the on-ground ISRF characterization, which typically prescribes measurements with partially illuminated slit widths. At any rate, instantaneous transitions are impossible be observed by any pushbroom instrument with finite FoV and integration time. Therefore they cannot be claimed to be representative for so-called "high-contrast missions" (which is not a defined category anyway).

Response: We agree, the description of the scene is missing and the derivation of it is not mentioned yet. We will include a description of the applied realistic test scene case, how it is designed and how we accounted for the slit smearing due to the satellite motion. The data for the scene is referring to the Type-2 scene of the Sentinel-5/UVNS System requirement document (Sentinel-5 UVNS Instrument Phase A/B1 Reference Spectra) and represents the scenes, under which the SH has to reduce the contrast in alignment with the mission requirements. We agree that Sentinel-5 may observe scenes with higher contrasts, which are however excluded from the mission requirements. Therefore we propose to constrain our study to the mission requirements as defined by ESA and apply our SH model to the scenes defined in the SRD. The interpretation and justification of why the scenes defined in the SRD are representative of the Sentinel-5 mission are out of the scope of this paper.
We will revise the discussion on the stationary calibration scenes and how they are used in the Sentinel-5 project. As mentioned by the referee, the stationary calibration scenes are not a realistic scenario and will never be seen by the instrument in the presence of motion smear of the platform. We will mention the stationary calibration scenes for the purpose of on-ground SH performance verification.

Changes in manuscript: The derivation and explanation of the applicable Earth scene for the Sentinel-5/UVNS mission is given in section (3) (lines 214-232). Note that we changed the name from "S5-ESA-Scene" to "applicable Earth scene". The discussion of the application of the calibration scenes is also given in section (3) (lines 233-236). We also mention in the newly established "Results and discussion" section, that extreme albedo variations are excluded from the Sentinel-5/UVNS mission requirements (line 339) and in Section 6 (line 374).

R2: **3. Unclear, somewhat arbitrary assumptions on imaging aberration, which partly invalidates the applicability of the results to the instrument under investigation (Sentinel-5).[...]**
For the propagation of the non-uniform pupil illumination pattern to the focal plane, aberration theory is used, describing the various types aberration with Zernike polynomials. While this is an adequate approach, the derivation of Zernike coefficients appears odd. It is claimed that the aberration components of the Sentinel-5 instrument are unknown, which seems surprising given the long history of design and development work (starting 2010). Instead, two aberration types are presented (spherical and comatic), without further explanation why they are selected to represent the instrument. The coefficients are derived by fitting the width of the PSF to the expected Gaussian (from optical analysis), implying that only one type of aberration is present and accounts for the entire PSF width. While this approach may be useful to qualitatively indicate the criticality of different types aberration, it does not appear representative for the Sentinel-5 instrument (as implied by the manuscript title). The strong dependence on the shape of the PSF, which seems to govern the wide range of ISRF errors, raises the question if the results can be used to predict the ISRF performance for a (more realistic) combination of the investigated aberrations.

Do the ISRF-shape errors for spherical and comatic errors (reported in tables 1-3) add up linearly or RSS in systems with both aberrations ? The authors shall... 1a) perform analysis with the estimated aberrations of the Sentinel-5 instrument (NIR and SWIR bands), or 1b) justify more clearly why such estimate of Sentinel-5 (in the NIR band) cannot be made. 2) in case of 1a) perform various analysis with cases of mixed aberration to explore the how different aberration components add up 3) if possible, extend the analysis to other types of aberration

Response: The aberrations present in the Sentinel-5/UVNS will vary with wavelength and ACT field point. Further, they will not be characterized experimentally but only in terms of RMS spot size. Although not a realistic case, it was our intention to investigate how different PSF, based on a pure single aberration component, impact the ISRF stability. Therefore, the analysis was intended to be representative in RMS spot size, but not in terms of the exact RMS wavefront error. In the revised manuscript, we will change the analysis to additional Zernike terms and also include mixtures of expected aberrations in Sentinel-5/UVNS and investigate how the different aberration components add up to the overall ISRF knowledge.

Changes in manuscript: We extended the analysis to several other Zernike Polynomials including two mixtures consisting of three individual Zernikes. The motivation and explanation for the Zernike analysis is given in line 298-306. The results of the analysis are given in Table (1) and (2).

R2: **4. Lack of exploitation of the obtained results (no comparison with classical slit, no flowdown of the results to Level-2 performance, missing interpretation in terms of implications for design improvements).[...]**
The final results are presented in three tables, in which the three figures-of-merit (shape distortion, FWHM and spectral barycentre position) are listed for three assumed aberration scenarios and four selected scenes. The interpretation is limited to commenting on the values listed therein, reporting the expected higher values for higher contrast, the difference between the three aberration cases, and the large values for the CAL-scenes. The latter are found to be are alarmingly high, but no conclusions are drawn for the instrument under investigation. It is merely stated that the performance is compliant for the "S5-ESA-scene", which is not surprising as it features very low contrast. The reader is left clueless about the real performance for higher contrast scenes, or complex albedo variation which the instrument will be exposed to in flight. In fact, it is not even clear if the use of a SH brings any advantage over using a classical entrance slit. It would be important to clarify if the performance gain by homogenisation of the near-field is completely or only partially lost by the induced far-field non-uniformity. No plots of the distorted ISRFs are provided, which would be instructive for the prediction of the impact on retrieved products. It would be interesting to see, how the different types of aberration affect the ISRF for the various scenes (e.g. extension of the wings or skewing the shape). While the changes are probably too subtle to be seen in the ISRF, it should not be difficult to include difference plots w.r.t. the homogeneous reference for some (extreme) cases. It should even be possible to flow down the obtained ISRF distortions to the Level-2 products. This is not easy in absence of a Level-2 processor (or end-to-end simulator), but could be approximated by using so-called gain vectors, which are part of the Sentinel-5 requirement definition. It would also be insightful to present the radiometric errors arising from the distorted ISRFs, at least for the extreme cases (largest and lowest). For this, the monochromatic reference spectrum would be convolved with the obtained (distorted) ISRFs and the difference plotted as a fraction of the true radiance (homogeneous, aberration-free case). The manuscript also falls short on providing implications of the results, and recommendations for design improvements. Can the pupil non-uniformity from SH be limited by design or is it an unchangeable "fact-of-life" ? Does it depend on the number of reflections and

can be mitigated by extending of SH along the optical axis? How important is the slit width and the focal lengths of the telescope and collimator ? Can the results be used to guide the optical design of the collimator and imager optics, e.g. regarding the types of aberration ?

Response: We agree, the interpretation and conclusions of the result are very limited. In the revised manuscript, we will add a more thorough discussion. We will compare our results to the case with a classical slit and highlight the improvement of the scene homogenization even in the presence of spectrograph illumination variations. We will also point out, that the calibration scenes for which we calculate the ISRF merit functions are only representative of on-ground measurements and don't represent real flight scenarios. As it should be the primary goal of this study to compare with real flight scenarios, we would only present a single Calibration Scene (50%) and emphasize, that the values obtained are without accounting for motion smear and therefore yield exaggerated ISRF distortions.
We will include plots of the distorted ISRF for different types of aberrations and also compare to the case of using a classical slit.
The flow down of the obtained ISRF distortions to Level-2 products is definitely important. We are currently working on another study dedicated to assess the improvement of Level-2 products by employing a slit homogenizer. Therefore, we will publish this topic in a subsequent publication. We will also add a discussion about design recommendations.

Changes in manuscript: We added the "Results and discussion" section (Sect. 5) (lines 309-365).

R2: **5. Invalid conclusions about other missions, which use different SH technology, and based on inadequate comparison of mission requirements.[...]**
Two main conclusions drawn by the authors are poorly justified: Conclusion 1): Quote: "A representative scene of the Sentinel-5/UVNS instrument has a rather weak contrast and therefore the instrument fulfils the ISRF specifications in order to meet the Level-2 performance requirements of the mission. In contrast to this, future missions like CO2M have to be compliant with higher contrast scenes with almost a sharp transition from dark to bright slit illuminations." Both parts of the above conclusion... a) There is no criticality for Sentinel-5 as it will only see low contrast b) CO2M will experience large errors, because it will see much larger contrast ...cannot be justified by the presented analysis: a) The low-contrast scene for Sentinel-5 (no source and details given) is likely from the system requirement document (please confirm). Such reference scenes are often specified to constrain individual error sources (e,g, straylight), but do not necessarily represent realistic geophysical scenarios. It appears certain that a Sentinel-5 measurement in the SWIR band near water bodies (coast lines or lakes), with an instantaneous field-view of 2.5 km smeared over 7.5 km will yield much larger effective contrast than the scene referred to as "S5-ESA-scene". b) CO2M is not a "high-contrast mission" as opposed to Sentinel-5. All nadir-looking pushbroom spectrometers look at the same Earth scenes, and the effective scene contrast observed over the integration time depends on the ratio of the slit projection and the ALT sampling distance. This ratio is comparable for bot, S5 and CO2M, and therefore the "smearing" of the contrast will be similar (not a sharp transition as claimed). The formulation of requirements by means of contrast scenes is often driven by straylight requirements, which may be more stringent for CO2M (due to deeper absorption structures in the SWIR-2 around 2.0 µm). However, such contrast scenes cannot be regarded as "representative Earth scenes". In case of CO2M the specified scenes exhibit an extreme albedo contrast (factor of 8) that is only observed over coast lines (and then mitigated by motion smear). The authors should refrain from performance prediction based on the interpretation of requirement documents, especially for missions out of the scope of this investigation (see below). Conclusion 2): Quote: "The application of the slit homogenizer

for missions with high contrast scenes (CO2M) will impose strong variations in the spectrograph pupil and will result in large errors in the ISRF and hence significantly degrades the accuracy in the retrieval of the atmospheric composition and therefore the mission product." This speculative statement is most likely false for the following reasons (on top of the ones given above): a) The presented model for ISRF distortions is based on waveguide propagation along a mirror-based SH. Such a device is not foreseen for CO2M, where a fibre based slit will be employed instead. The model developed in this paper is not valid for light propagation in multimode fibres. In fact, measurements of transfer functions with such a fibre based, twodimensional slit homogeniser (2DSH) have not shown interference patterns as shown in Fig. 3b. (see S.Amann et al., Characterization of fiber-based slit homogenizer devices in the NIR and SWIR, Proceedings Volume 11180, International Conference on Space Optics — ICSO 2018; 111806C (2019) https://doi.org/10.1117/12.2536147 b) Scene-dependent far-field effects from scene non-uniformity are also expected for fibre slits, but are typically less pronounced and can be mitigated by adjusting the fibre length (see G. Avila, "FRD and scrambling properties of recent non-circular fibres," Proc. SPIE 8446, Ground-based and Airborne Instrumentation for Astronomy IV, 84469L (24 September 2012); doi: 10.1117/12.927447). They are related to the fibre modes and are expected to show lower frequency variations than the ones found in this study. They can also be mitigated by fibre bending. It is understood that the authors seek to underline the importance of their results by pointing out the relevance to other missions. While this is legitimate, CO2M is not an appropriate mission for comparison. I am aware of only one other mission considering the implementation of a mirror-based SH: The Geostationary Carbon Cycle Observatory (GeoCarb), which is not quoted in the manuscript. Its step-and stare slit-scan strategy is likely to be more critical regarding the discussed effects than Sentinel-5, because of the absence of motion smear. Unless the authors can justify the validity of their propagation model for rectangular multimode fibres, it is suggested to remove speculative statements about CO2M's in-orbit ISRF stability performance. Instead it is proposed to make reference to GeoCarb (and make the team aware of a potential error source not yet considered), e.g.: - B.Moore, "The GeoCarb Mission," in 14th International Workshop on Greenhouse Gas Measurements from Space, (2018) - J. Nivitanont et al: Characterizing the Effects of Inhomogeneous Scene Illumination on the Retrieval of Greenhouse Gases from a Geostationary Platform. Poster presented at the 4th International Workshop on Greenhouse Gas Measurements from Space, (2018) Finally, I propose to add a conclusion that is currently missing: Both, the transfer function shown in Fig. 3b, as well as the pupil intensity distributions in Fig. 6 should be accessible to measurement employing an appropriate test bench. It is assumed that the two SH devices in Sentinel-5 are now mature enough to be tested (btw. please note the existence of two different such slits in the manuscript). Far-field measurements with these devices could be used to verify the derived model, and to quantify the ISRF errors expected from measured pupil intensity variation. If the authors agree, I suggest to include such proposal and give indications on how to implement an appropriate measurement.

Response: We agree and remove the conclusion and connections that we tried to establish to the CO2M mission. Our intention was to point out the limitations of the 1D-Slit Homogenizer in terms of scrambling performance over extreme albedo contrasts. However, as mentioned by the referee, CO2M is not employing a mirror based slit homogenizer but a fibre-based 2DSH and our model is not applicable to such devices.
We follow the referee's recommendation and include a suggestion on how to experimentally verify the expected pupil intensity variations.

Changes in manuscript: The references to the CO2M mission have been entirely removed from the manuscript. We briefly mention the work on another scene homogenization techniques based on multimode fibres (lines 362-365.). The experimental suggestion for a dedicated measurement setup to experimentally verify our simulation results is given in lines 355-361.

2.2 Technical corrections / Editorial Comments

R2: **1. p. 1; "The spectral accuracy" is not well defined so far.**

Response: We will change the sentence.

Changes in manuscript: see lines 1-3.

R2: **2. l. 3-5: "As the ISRF is the direct link between the forward radiative transfer model" >> add: ", used to retrieve the atmospheric state..."**

Response: Done.

Changes in manuscript: see lines 3-4.

R2: **3. l. 14: "By homogenizing the slit illumination, the SH moreover strongly modifies the spectrograph pupil as a function of the input scene" >> insert "illumination" after "pupil"**

Response: Done.

Changes in manuscript: see line 14.

R2: **4. l. 16: "type" >> "type"**

Response: Probably it is meant to change it to "types" which will be done.

Changes in manuscript: see line 16.

R2: **5. l. 19 "As in most space based imaging spectrometer" >> is too general, e.g. imaging FTS (e.g. IASI) are not affected (no slit) Also indicate the difference to scanning spectrometers, like SCIAMACHY**

Response: We will point out the difference to imaging FTS and scanning spectrometers.

Changes in manuscript: see lines 20-23.

R2: **6. 20: "spectrometer" >> "spectrometers"**

Response: Obsolete due to new formulation above (6.)

R2: **7. l. 20: "gets imaged" >> "is imaged" (is the purpose)**

Response: Done.

Changes in manuscript: see line 20.

R2: **8. l. 21: delete "eventually"**

Response: Done.

R2: **9. l. 22: "gets convoluted" >> "is convolved"**

Response: Obsolete due to new formulation below (10.).

R2: **10. l. 22: better: "The limited spectral resolving power of the instrument arising from diffraction and aberration is describe by a convolution of the slit image with the spectrometer and detector point spread functions (PDF).**

Response: Done.

Changes in manuscript: see line 23-25.

R2: **11. l. 24: " The resulting intensity pattern on the FPA in the spectral direction is called the instrument spectral response function (ISRF)." − > This is not a universal definition. According to ESA definition, this is the ISMF (Instrument Spectral Measured Response), which is not measurable continuously, but sampled by the detector pixels. ESA defined ISRF for each detector pixel as a continuous function of wavelength, defined as the individual pixel's response at a given wavelength. In absence of aberrations, this ISRF is a mirror of the ISMF (inverted on the spectral scale), but in reality this is not the case. For definitions please refer to : Caron, J., Sierk, B., Bézy, J.L., Löscher, A., and Meijer, Y., The CarbonSat candidate mission: Radiometric and spectral performances over spatially heterogeneous scenes, Proceedings of the International Conference on Space Optics (ICSO), Tenerife, Spain, 2014**
It is also suggested that the authors read and (if found appropriate) cite the following reference, which highlights the issue of inhomogeneous slit illumination for a relevant airborne instrument: Gerilowski, K., Tretner, A., Krings, T., Buchwitz, M., Bertagnolio, P. P., Belemezov, F., Erzinger, J., Burrows, J. P., and Bovensmann, H.: MAMAP – a new spectrometer system for column-averaged methane and carbon dioxide observations from aircraft: instrument description and performance analysis, Atmos. Meas. Tech., 4, 215–243, https://doi.org/10.5194

Response: We will soften the formulation and indicate, that in our the model, the ISRF is defined as the slit intensity pattern on the FPA in the spectral direction. We will add the reference to the proposed paper and indicate, that our definition is only valid in the absence of smile effects.
We will also cite the paper of Gerilowksi et. al in the discussion of non-uniform scenes in ACT direction.

Changes in manuscript: For the definition of the ISRF, see lines 25-28.
The citation of Gerilowski et al. in the context of non-uniform scenes in ACT is given in lines 67-69 and 230-231 .

R2: **12. l. 28: "Figure 2 depicts a representative Top- of-Atmosphere spectrum" >> Be more specific, indicate the albedo and SZA.**

Response: Done.

Changes in manuscript: see line 33.

R2: **13. l. 28: "in the SWIR wavelength band" − > "for the Sentinel-5 SWIR-3 spectrometer, used for retrieval of CH4 and CO" >> The plotted spectral band is one out of 2 SWIR bands of the Sentinel-5 mission, and other missions have yet different**

band definitions.

Response: Done.

Changes in manuscript: see line 34.

R2: **14. l. 29: "entering a space-borne instrument" − > "incident on a space-borne instrument's entrance aperture" "high-resolution" − > "monochromatic" or "unconvolved"**

Response: Done.

Changes in manuscript: see line 34-35.

R2: **15. l. 30: "for every monochromatic stimulus" Not clear what is meant by this. It seems to refer to the incident spectrum as a continuum of monochromatic stimuli. Better replace by "for any given wavelength"**

Response: Done.

Changes in manuscript: see line 36.

R2: **16. l. 31 "Whenever the ISRF shape deviates from the on-ground characterized shape..." while the ISRF has been introduced as a mathematical convolution kernel, on-ground characterisation is mentioned "by the way" in a side sentence. It should be mentioned in the text that the ISRF is a wavelength- and field-of-view dependent instrument characteristic (varying with wavelength and ACT field position), and is determined by onground characterisation prior to launch.**

Response: We will add the FPA position dependent ISRF characteristics and the on-ground characterization prior to launch.

Changes in manuscript: see lines 36-39.

R2: **17. l. 32 "..., which serves as a basis for the applied retrieval algorithms." − > "...from which the Level-2 products are retrieved". (measurements are the input to, not the basis of an algorithm). Since the paper mainly addresses the Sentinel-5 mission and the SWIR bands, the retrieved Level-2 products shall be mentioned (CH4, CO columns).**

Response: Done.

Changes in manuscript: see line 40.

R2: **18. l. 33: "The along track motion of the satellite accounting for the spectral direction of the spectrometer serves as an averaging and smearing effect of the scene" "The along track motion of the satellite during the integration times results in a temporal averaging of the ISRF variation, which reduces the impact of scene heterogeneity." Also mention here that the impact of albedo variations depends on the ratio of the instantaneous field-of-view (IFOV) and the sampling distance in ALT. Please indicate these numbers for Senyinel-5 (FoV=2.5km, ALT SSD = 7.5km).**

Response: Done.

Changes in manuscript: see lines 41-44.

R2: **19. l. 36: "are less vulnerable to contrast in the Earth scene" − > Indicate the reason: The effect depends on the ratio of spatial sampling distance (in this sentence "scan area"), and the instantaneous field of view (see comment above)**

Response: We will add this information.

Changes in manuscript: see lines 45-46.

R2: **20. l. 36: "In contrary," − > in contrast**

Response: Done.

Changes in manuscript: see line 46.

R2: **21. l. 37: "...define a set of stringent requirements on the inflight knowledge and stability of the ISRF." >> add the reasone before: "...high resolution hyperspectral imaging spectrometers with IFOV comparable to the sampling distance (or scan area) are more strongly affected and therefore define..."**

Response: Done.

Changes in manuscript: see lines 46-47.

R2: **22. l. 38: "will introduce biases in the Level-2 data" add "and pseudo-random noise" after "biases", which is actually the main impact over an ensemble of measurements.**

Response: Done.

Changes in manuscript: see lines 48-50.

R2: **23. l. 39: "For the 2017 launched Sentinel-5 Precursor (S5P) satellite..." − > "For Sentinel-5 Precursor (S5P) satellite, launched in 2017,", and add reference for mission description, e.g. J. P. Veefkindet al., TROPOMI on the ESA Sentinel-5 Precursor: A GMES mission for global observations of the atmospheric composition for climate, air quality and ozone layer applications, Remote Sensing of Environment, Volume 120, p. 70-83 (2012)**

Response: Done.

Changes in manuscript: see line 50-51.

R2: **24. p. 3; Figure 2: >> Suggested to plot the monochromatic TOA spectral radiance and the convolved, simulated measurements should be plotted here as well.**
>> Briefly explain the origin of the spectral structure, indicating the absorption features by CH_4, CO, and H_2O.
>> It would be instructive to include an over-plot of a spectrum with distorted ISRF for a realistic scene contrast, and to include a difference plot w.r.t. the homogeneous case

Response: We add the explanation of the spectral structures.
The considerations about radiometric errors due to ISRF distortions in the context of non-uniform

scenes will be presented in a subsequent study. For this manuscript we will focus on the ISRF knowledge in terms of the figures of merit as defined in the manuscript and hence will not go into further detail about the variation of the spectra for different ISRFs.

Changes in manuscript: see caption of Figure 2.

R2: **25.l. 43: "Noel et al. (2012) quantify the retrieval error for the Sentinel-4 UVN imaging spectrometer for the tropospheric O3, NO2, SO2 and HCHO." >> Indicate that Sentinel-4 is not yet launched (adding "upcoming") and that these results are based on simulations, not real measurements (in contrast to the TropOMI results quoted before). Also introduce the not yet defined acronym "UVN".**

Response: Done. The acronym UVN will be added, where mentioning Sentinel-5/UVNS for the first time.

Changes in manuscript: see line 34.

R2: **26. l 45: "They propose a software correction algorithm which is based on a wavelength calibration scheme individually to all Earthshine radiance spectra" - add comma in $->$ "algorithm, which..." - add "applied" and replace "Earthshine" by "Earth" (even though used in the reference)$->$ "...individually applied to all Earth radiance spectra..."**

Response: Done.
Changes in manuscript:see lines 57-58.

R2: **27. l. 49,50: "...to mitigate the effect of non-uniform scenes." add "in along-track direction", as the S5's SH only homogenises in ALT. It shall be mentioned, that non-uniform scenes in ACT direction also result in ISRF distortion in presence of smile distortion in the image plane. This is e.g. explained in the already quoted Caron et al. 2014 (see reference above).**

Response: We will mention the impact of heterogeneous scenes in ACT direction and refer the reader to Gerilowski et. al (2011) and Caron et al. (2017).

Changes in manuscript: see lines 67-69 and 230-231.

R2: **28. l. 51: move "in the along track direction (ALT) of the satellite flight motion" after "Earth radiance"**

Response: Done.

Changes in manuscript: see line 63.

R2: **29. l. 53: "...mirrors is of b = 240 µm (NIR)," $->$ replace "of" by "has dimensions of" Proposed: "The two parallel rectangular mirrors composing the entrance slit have a distance of b = 240 µm (NIR), side lengths of 65 mm in ACT and a length of 9.6 mm along the optical axis".**

Response: Done for the values in the SWIR-3 channel.

Changes in manuscript: see line 65.

R2: **30. l. 54: "gets scrambled" $->$ "is scrambled by multiple reflections"**

Response: Done.

Changes in manuscript: see line 66.

R2: **31. l. 55: "For a realistic reference Earth scene of the Sentinel-5/UVNS mission" >> Please indicate the specifics of the scene (albedo image or artificial contrast)?**

Response: We will revise the whole section of the description on the applied scene cases and refer to the answer in General Comment (2).

Changes in manuscript: See section (3), lines 214-230.

R2: **32. l. 56: "the total in orbit ISRF shape error budget is < 2 %, the relative Full width half Maximum (FWHM) error < 1 % and the centroid error in the NIR 0.02 nm" >> Although hidden in the word "budget" state more clearly that these are requirements, not resulting performances.**

Response: Done.

Changes in manuscript: see line 70.

R2: **33. l. 61: " We present an end-to-end model of the Sentinel-5/UVNS NIR channel (760 nm)." Please justify why the model (resp. its application) is restricted to the NIR band. Also replace, or add equivalent plots of the NIR band, as for SWIR in Fig. 2.**

Response: As we will change the analysis to the SWIR-3 channel, we assume that this comment becomes obsolete.

Changes in manuscript: The discussion on why the SWIR-3 is the most critical one is given in lines 342-344.

R2: **34. l. 63: "consequently implies a scene dependency in the optical PSF" "implies" $->$ "results in"**

Response: Done.

Changes in manuscript: see line 78.

R2: **35. l. 65: "spectrograph pupil intensity distribution" $->$ "intensity distribution across the spectrograph pupil"**

Response: Done.

Changes in manuscript: see line 79-80.

R2: **36. l. 76: "contains details" $->$ "describes"**

Response: Done.

Changes in manuscript: see line 91.

R2: **37. l. 78: "The second part focusses on the novel modelling technique of the spectrograph optics." Not understood. Is "novel modelling technique" referring to the previous sentences, or is it announcing a new technique to be established in the paper. In the latter case, better write: "In the second part a novel modelling technique of the spectrograph optics is introduced".**

Response: Here we wanted to refer to the technique established in the paper. Therefore we will use the recommendation as proposed by the Referee.

Changes in manuscript: see line 93-94.

R2: **38. l. 87: Please mention that equation 2 follows from equation 1 with the simplifying assumption of a square entrance pupil. This is currently hidden in a side remark on line 92. Clarify the calculated quantity $\tilde{U}_f, \theta$ (electrical field?), currently referred to as "the Airy disk"**
>> Please clarify if this propagation model has been verified against measurements of the SH transfer function.
Caption of Fig. 3 "...highly dependent on interference effects" $->$ "are strongly affected by interference effects, resulting in a complex illumination pattern at the slit exit". You should mention that this is not a new finding, but a known characteristic of such SH device, and that the interference pattern, although not uniform, already represents an improvement over no scrambling in a classical slit.

Response: We will add a sentence and mention that the airy disc is the field distribution in the slit plane and is given by the Fourier transform of the electric field over the entrance pupil. As the telescope pupil is actually of rectangular shape, we will change the word airy pattern to diffraction pattern.
We will mention, that a full end to end verification of the propagation is still missing. However, an initial approach by ITO Stuttgart to validate the performance model in a breadboard activity gave confidence on the approach of the optical model (see Irizar et al. (2019)).

Changes in manuscript: The explanation of the airy disc is given in lines 101-102. Note that we changed the formulation from airy disc to diffraction pattern.
The reference to the measurements of ITO Stuttgart Published in Irizar et al. ar given in lines 123-124.
We provide a thorough comparison to a classical slit in the Section (5) and also discuss the limitation of the SH based on the remaining fluctuations of the SH transfer function.

R2: **39. l. 121: ". Independent of the applied scene in ACT, the telescope pupil is retrieved again at the spectrograph pupil despite a magnification factor and a truncation of the electric field at the SH entrance plane, which leads to a slight broadening and small intensity variations with a high frequency in angular space (Berlich and Harnisch, 2017)." >> split in 2 sentences**
Figure 4.: Indicate in the caption the astigmatism of the collimator, which is adjusted to the slit length.

Response: Done.

Changes in manuscript: see caption of Figure 4.

R2: **40. l. 134: "...spectrograph pupil will be altered with respect to the telescope pupil" The manuscript frequently refers to "altering" telescope and spectrograph pupils, although these are optical-geometric terms that do not depend on the illumination. For better correctness it should be rephrased in terms of "pupil illumination "**

Response: We corrected the respective formulations throughout the manuscript.

R2: **41. l. 134: "A general case for the connection between slit exit plane and spectrograph pupil plane is considered by Goodman (2005, p. 104)" The coordinates in Eq. 5 seems to be for the slit exit and spectrograph pupil, respectively, which differs from Eq. 2-3, where x,y, denote coordinates in the telescope pupil and u,v those in the slit exit. Please clarify the coordinates or use indices to indicate the difference.**

Response: We agree, that our notation is confusing. We changed our coordinate notation in the following way: x_t, y_t are the coordinates at the telescope pupil, u_a, v_a at the SH entrance plane, u_b, v_b at the SH exit plane and x_s, y_s at the spectrometer pupil plane. Note, that we also observed a typo in equations (5,6,10), which was the incorrect factor $(u^2 + v^2)$ in the integral.

Changes in manuscript: We changed the coordinate formulation throughout the manuscript. Note that we also observed small typos in equation (4),(5),(10),(14) and (17) which are showed in the changelog of the manuscript at the end of the document.

R2: **42. l. 139: "where k is the wavevector of the incoming wave, λ is the wavelength and f is the focal length of the lens" Quantities already defined above.**

Response: We erased the sentence.

R2: **43. l. 144, Eq. 6: Is it necessary or convenient to keep 2pi and lambda in the argument of the field distribution ?**

Response: It was our intention to highlight the coordinate transformation that was necessary in order to solve the equation. In the revised version we define: $x_s' = \frac{2\pi}{\lambda f} x_s$ and $y_s' = \frac{2\pi}{\lambda f} y_s$.

Changes in manuscript: We introduce the coordinate transformation in line 188.

R2: **44. l. 145: By ending the section with an uncommented equation, the reader is left with the question what is the conclusion so far (or the purpose of the calculation). It should be noted that this is an intermediate result, which will be further propagated and refined in the following (for collimator astigmatism).**

Response: We will add a comment on the derived formulation.

Changes in manuscript: see lines 168-169.

R2: **45. l. 162: " straight forward" $->$ "straightforward"**

Response: Done.

Changes in manuscript: see line 182.

R2: **46. l. 175: " Further, we model the dispersive element as a 1D binary phase diffraction grating." >> Indicate if this choice is relevant to the actual Sentinel-5 instrument. An image of the binary grating structure would be useful here (also for explaining the quantities used in the text).**

Response: We will add an explanation, that the used model for the grating is a simplified assumption. We will add the real grating configurations of the Sentinel-5/UVNS in the SWIR-3.

Changes in manuscript: see line 209-211.

R2: **47. l. 191: "...representative Earth scene for the Sentinel-5/UVNS instrument provided by ESA (S5-ESA-scene)..." The "scenes" referred to here need to be further described. Is it the artificial contrast scene (bright and dark reference spectrum)? In that case they should not be called "representative Earth scene", but a step transition scene with contrast factr representative for the mission requirements.**

Response: We will revise the whole section and refer to the answer in General Comment (2).

Changes in manuscript: see Sect. 3.

R2: **48. l. 194: "Fig. 5 shows the top of atmosphere (ToA) radiance level given by a realistic Earth scene for the Sentinel-5/UVNS instrument." This is likely showing the contrast for one wavelength (supposedly spectral continuum level), which can vary significantly across the spectrum (zero in case of saturation). Please clarify in the text.**

Response: We will revise the section and refer to the answer in General Comment (2).

Changes in manuscript: see Sect. 3.

R2: **49. l. 195: "Due to smearing of the satellite's movement, this scene has a significantly lower contrast than the calibration scenes"**
>> Indicate this by plotting the convolution of the contrast with a boxcar function of the motion smear, which would show the contrast the instrument sees during integration time.

Response: This will be done in the revised section (see General Comment (2)).

Changes in manuscript: See Figure 5.

R2: **50. l. 196-200: The remark about the CO2M seems misplaced here, and should be moved to the discussion of the results (if maintained at all). It seems incorrect to equate a "calibration scene" with stationary contrast in the slit with a "representative scene of another instrument (especially with a different type of SH, see below). While it is true that nonhomogeneous scenes are more critical for CO2M, there will also be smoothing by morion smear, and a sharp transition cannot be observed. This is different from step-and-stare instruments (e.g. GeoCarb), which could be mentioned here.**
Fig. 5: It is still unclear, how the relatively flat "S5-ESA-scene" was derivedn(origin and processing, e.g. convolution with motion smear, assumption of slit projection, etc.). Please clarify.

Response: We removed the reference to CO2M (see General Comment (5)).
The derivation of the scene will be explained in more detail in the revised version of the manuscript (see answer to General comment(2)).

Changes in manuscript: For the derivation of the scene, see Sect. 3.

R2: **51. l. 201: "Figure 6 depicts the pupil intensity distribution in the NIR (760 nm) for the applied test scenes" >> Indicate that these are simulations based on the equations derived before.**

Response: We will indicate that the results are based on simulation.

Changes in manuscript: See caption of Figure 6 and line 236.

R2: **52. l. 202: remove "is happening" $->$ "due to the absence of interaction, i.e. reflection, with the SH"**

Response: Done.

Changes in manuscript: see line 238.

R2: **53. l. 204: "retrieved" $->$ "preserved"; "Contrary" $->$ "In contrast"**

Response: Done.

Changes in manuscript: see line 239.

R2: **54. l. 215: "We know from ray tracing simulation predictions the PSF size on the FPA of the Sentinel-5/UVNS NIR channel, which in a simplified model is given by the standard deviation of a normal distribution.As the actual aberrations present in the system are yet unknown,..." $->$ It is hard to believe that the aberrations for the Sentinel-5 instrument are completely unknown at this point (so far into the project).The PSF usually depends on field position (and wavelength), and should be well characterised by the optical analysis. It is understood that the use of Gaussians is convenient for the mathematical analysis, but it would be good to verify the results are robust against more representative PSF.**

Response: See General Comment (3).

Changes in manuscript: As mentioned above in General Comment (3).

Eq. 14: - Explain that (u,v) are now the coordinates at the focal plane - The intensity I_{theta} is the square of the absolute value of U_{FPA}, which has no dependence on theta in Eq. 14. Please clarify why it appears as a function of theta in Eq. 15. It might be good to write here the one-dimensional equation for $I(\theta,\nu)$, as it represents the final result for the ISRF distortion.
It is not clear how the aberrations to demonstrate the impact of inhomogeneous pupil illumination were selected (randomly, analysis or for convenience) ? It should be possible to make realistic estimates on the aberrations present in the Sentinel-5 instrument. This would enhance the credibility of the results regarding ISRF impact.

Response: In order to avoid confusion we change (u,v) to (s,t) and mention that they are the coordinates at the FPA plane.
In the derivation of the field distribution of the SH exit plane (Eq. 4) we indicated, that the calculation is made for a single incidence angle θ onto the SH entrance plane. As the referee rightly mentions, this reference was not made in the subsequent steps, which still describe the propagation of a single SH entrance incidence angle θ. It will be added to the equations describing the propagation through the spectrograph.

Changes in manuscript: See new formulation of the coordinates in line 267.
For better reading, we erased equation (6) of the previous version of the manuscript and mention it directly in equation (9) of the revised manuscript. The angle θ was added accordingly to equation (9,11,12,14).

R2: **55. l. 262: "result" – > "results"**

Response: Obsolete due to new formulation.

Changes in manuscript: see lines 291-295.

R2: **56. l. 264: << "As a direct comparison of the difference between an ISRF calculated with a PSF disturbed by aberrations and a PSF given as a pure normal distribution is problematic, we rather compare the errors relative to a homogeneous scene." >> Please explain in more detail why it is "problematic". It was stated above that assuming a Gaussian PSF would "neglect the non uniformity in the pupil and the spectrometer aberrations."**
Table 1-3: - It is not clear why the errors are so large for the Gaussian PSF case. If the ISRF distortion originates from scene-dependent weighting aberrations, then this case should not yield large errors. - Please indicate in the text how these results compare with the requirement for ISRF knowledge. - Please plot the distorted ISRFs corresponding to the results in the table (at least the extreme ones) - It is suggested to also include plots showing radiometric errors resulting from such distortions
>> Does the result, which predicts large ISRF knowledge errors from the "calibration scenes", have any implications on the on-ground calibration of the instrument? Please elaborate.

Response: A direct comparison of ISRF containing different kind of aberrations creates a systemic error as the ISRFs are based on different PSF (due to the different aberrations) and are not comparable even in the absence of non-uniform scenes. However, the ISRF will be extensively characterised on-ground for homogeneous scenes and hence aberrations are compensated by calibration. We want to investigate how the ISRFs based on several Zernike terms behave under the condition on non-uniform scenes and how the ISRF errors evolve with respect to each specific homogeneous ISRF. Therefore we calculate the relative change in ISRF figure of merit functions and not directly compare differently aberrated ISRFs with each other.
The errors presented in the tables represent the ISRF errors combining the effect of remaining SH exit non-uniformity (near-field) and non uniform spectrograph illumination (far field) in combination with optical aberrations. Therefore, the case of a constant gaussian PSF contains only the errors of the remaining near-field non-uniformity, whereas the case with Zernike aberrations and propagation through the spectrograph contains both, near field and far field errors. The relative difference in the ISRF stability between these two cases gives an estimation on the resulting far field errors contributions which is the main part of this study.
The previous version of the manuscript showed ISRF distortion values for calibration scenes that are used for the experimental validation of the SH performance model and don't represent real flight scenarios (see General Comment(2)). Therefore, the results are useful in the upcoming characterization and verification campaign to detect and understand possible discrepancies in the SH model and experimentally measured results for non-uniform scenes of such kind.
We will include plots of the distorted ISRFs.
As said in the response to General Comment (4), the investigations wrt the impact on Level-2 are ongoing and are planned to be published in a dedicated paper.

Changes in manuscript: We emphasize more clearly, that the errors shown in Table (1) and (2) are the combined errors of the near-field and far-field variations. See caption of Table (1) and line 296-297.
The plots of the distorted ISRF are given in Figure 7.
The application of the calibration scene is mentioned in lines 233-235 and 311-312.

R2: **57. l. 277: "gets significantly higher" – > "becomes significantly higher"**

Response: As we revise this section, this point becomes obsolete.

R2: **58. l. 279: "...comes only by..." $->$ "...comes only from..."**

Response: Obsolete as we revised the section.

R2: **59. l. 285: "A scene dependency of the spectrograph pupil will lead to similar ISRF distortion as due to non-uniform slit illuminations" >> This could, but was not shown here. The authors should provide calculations for ISRF distortions for a classical slit, in order to compare and support this claim.**

Response: We will compare the results with the case of a classical slit.

Changes in manuscript: The comparison with a classical slit is given in Table (1) and (2) as well as in Fig. 7a.

R2: **60. l. 281: "We also conclude, that for the Sentinel-5/UVNS instrument the impact of this effect is of second-order and doesn't degrade the performance of the SH significantly." This conclusion should be restricted to the reference scene used, not the Sentinel-5/UVNS instrument. Independent on the requirement formulation, the instrument might be exposed to larger contrast than used in this study.**

Response: See General Comment (2).

Changes in manuscript: See Sect. 3. We will mention, that larger contrasts scenes are excluded from the Sentinel-5/UVNS mission requirements in lines 336-338 and 372-373.

R2: **61. l. 328: Duplication in reference: Goodman, J. W.: Introduction to Fourier optics, Introduction to Fourier optics, 3rd ed., by JW Goodman. Englewood, CO: Roberts & Co. Publishers, 2005, 1, 2005.**

Response: Done.

Changes in manuscript: see line 425.

References

Irizar, J., Melf, M., Bartsch, P., Koehler, J., Weiss, S., Greinacher, R., Erdmann, M., Kirschner, V., Albinana, A. P., and Martin, D.: Sentinel-5/UVNS, in: International Conference on Space Optics — ICSO 2018, edited by Sodnik, Z., Karafolas, N., and Cugny, B., vol. 11180, pp. 41 – 58, International Society for Optics and Photonics, SPIE, https://doi.org/10.1117/12.2535923, URL `https://doi.org/10.1117/12.2535923`, 2019.

Slit homogenizer introduced performance gain analysis based on Sentinel-5/UVNS spectrometer

Timon Hummel[1,2], Christian Meister[2], Jasper Krauser[2], and Mark Wenig[1]

[1]Meterological Institute LMU Munich, Theresienstraße 37, Munich, Germany

[2]Airbus Defence and Space GmbH, Willy-Messerschmitt-Str. 1, 82024 Taufkirchen, Germany

Correspondence: Timon Hummel (timon.hummel@airbus.com)

Abstract.

~~The spectral accuracy~~ Spatially heterogeneous Earth radiance scenes affect the atmospheric composition measurements of high resolution Earth observation spectrometer missions~~is affected by the impact of spatially heterogeneous Earth radiance scenes on~~. The scene heterogeneity creates a pseudo-random deformation of the instrument spectral response function (ISRF). ~~As the~~ The ISRF is the direct link between the forward radiative transfer model, used to retrieve the atmospheric state, and the spectra measured by the instrument. Hence, distortions of the ISRF owing to radiometric inhomogeneity of the imaged Earth scene will degrade the precision of the Level-2 retrievals. Therefore, the spectral requirements of an instrument are often parametrized in the knowledge of the ISRF over non-uniform scenes in terms of shape, centroid position of the spectral channel and the Full Width at Half Maximum (FWHM).

The Sentinel-5/UVNS instrument is the first push-broom spectrometer that makes use of a concept referred as slit homogenizer (SH) for the mitigation of spatially non-uniform scenes. This is done by employing a spectrometer slit formed by two parallel mirrors, scrambling the scene in along track direction (ALT) and hence averaging the scene contrast only in the spectral direction. The flat mirrors do not affect imaging in the across track direction (ACT) and thus preserve the spatial information in that direction. The multiple reflections inside the SH act as coherent virtual light sources and the resulting interference pattern at the SH exit plane can be described by simulations using scalar diffraction theory.

By homogenizing the slit illumination, the SH ~~moreover~~ strongly modifies the spectrograph pupil illumination as a function of the input scene. In this work we investigate the impact and strength of ~~spectrograph pupil variations~~ the variations of the spectrograph pupil illumination for different scene cases and quantify the impact on the ISRF stability for different ~~type~~ types of aberrations present in the spectrograph optics.

1 Introduction

The Ozone Monitoring Instrument (OMI) was the first instrument identifying the issue arising from non-uniform Earth scenes on the shape and maximum position of the spectral response of the instrument (Voors et al., 2006). ~~As in most space based imaging spectrometer~~In slit based imaging spectrometers, the Earth ~~radiance scene gets~~ ground scene is imaged by the telescope onto the instrument entrance slit plane. The scanning over the ground area is achieved by either a scanning mirror or a push-broom configuration, where different areas of the surface are imaged as the satellite flies forward. In the subsequent spectrograph, the slit illumination gets spectrally resolved by a dispersive element and ~~eventually~~ re-imaged on the focal plane array (FPA) by an imaging system. ~~During the imaging process, the slit illumination intensity distribution gets convoluted by the spectrograph point spread function~~ The limited spectral resolving power of the instrument arising from diffraction and aberration is described by a convolution of the slit image with the spectrometer and detector point spread functions (PSF)~~and the detector pixel characteristics. The~~. In this study, we interpret the resulting intensity pattern on the FPA in ~~the spectral direction is called the instrument~~ spectral direction as the Instrument spectral response function (ISRF). In fact, there exist other definitions of the ISRF. The differentiation of the definitions become particularly important in the presence of spectrometer smile effects (Caron et al., 2017). As we neglect such effects, we will continue with the previously described definition of the ISRF.

Depending on the observed scene heterogeneity, the entrance slit will be inhomogeneously illuminated~~and~~. In the case of a classical slit, this will alter the shape of the ISRF (see Fig. 1). Moreover, a scene dependency in the PSF will also affect the ISRF, which will be particularly discussed in this manuscript. As the ISRF is the direct link between the radiative transfer model and the spectrum measured by the instrument, a scene dependent shape of the ISRF will have an immediate impact on the accuracy of the Level2-retrieval products. Figure 2 depicts a representative Top-of-Atmosphere spectrum ~~in the SWIR wavelength band, entering a space-borne instrument. The high-resolution~~ (SZA 10°, albedo 0.05) for the Sentinel-5/UVNS (Ultra-Violet/Visible/Near-Infrared/SWIR) SWIR-3 spectrometer, incident on the instrument's entrance aperture. The monochromatic spectrum will be smeared by means of a convolution with an exemplary ISRF, which depends on the imaging properties of the instrument for ~~every monochromatic stimulus. Whenever the~~ any given wavelength. In general, the ISRF is a wavelength and field-of-view dependent instrument characteristic and hence varies over the FPA position. It is experimentally determined prior to launch in on-ground characterization campaigns. Whenever the in-orbit ISRF shape deviates from the on-ground characterized shape, due to for example heterogeneous scenes, it will affect the measured spectrum, ~~which serves as a basis for the applied retrieval algorithms.~~from which the Level-2 products are retrieved (e.g. CH_4 and CO in the SWIR-3 channel of Sentinel-5/UVNS).

This effect is particularly prominent for instruments with a high spatial resolution. The along track motion of the satellite ~~accounting for the spectral direction of the spectrometer serves as an averaging and smearing effect of the scene.~~ during the integration times results in a temporal averaging of the ISRF variation, which reduces the impact of scene heterogeneity. The impact of e.g. albedo variations depends on the instantaneous field-of-view and the sampling distance in ALT (for Sentinel-5/UVNS: FoV = 2.5 km, ALT SSD = 7 km). Spectrometers with a large scan area like GOME (Burrows et al., 1999) or ~~SCHIAMACHY~~ SCIAMACHY (Bovensmann et al. (1999), Burrows et al. (1995)) are less vulnerable to contrast in the Earth scene ~~. In contrary~~due to the small ratio between the slit footprint and the smear distance. In contrast, recent high resolution hyperspectral imaging spectrometer ~~define~~ with IFOV comparable to the sampling distance (or scan area) are more strongly affected and therefore demand a set of stringent requirements on the inflight knowledge and stability of the ISRF. This is necessary, as distortions in the ISRF due to non-uniform scenes will introduce biases and pseudo-random noise in the Level-2 data and therefore in the precision of atmospheric composition products. For ~~the 2017 launched~~ Sentinel-5 Precursor (S5P) satellite

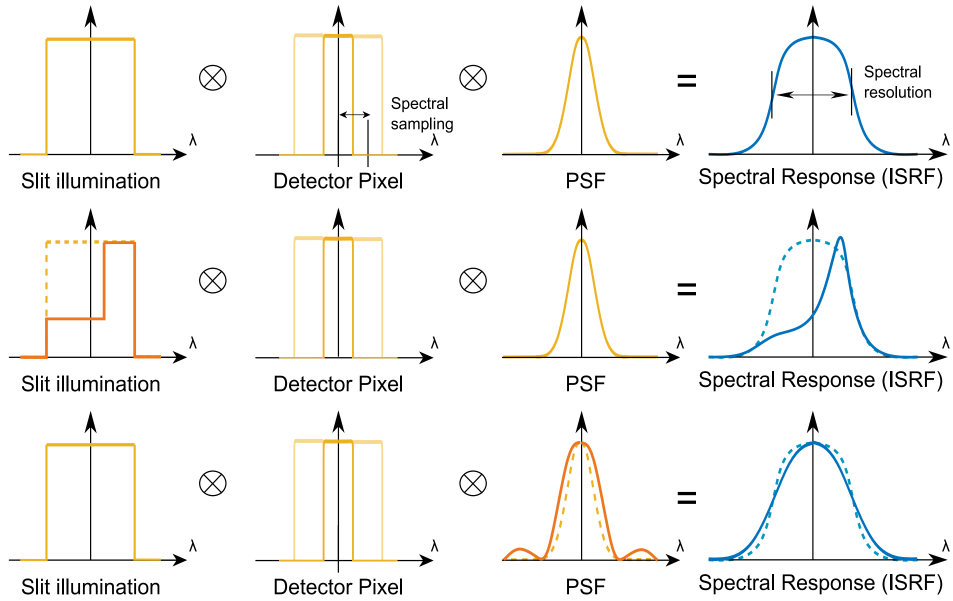

Figure 1. The ISRF of an imaging spectrometer is given by the convolution of the slit illumination, pixel response and the optical PSF of the spectrograph optics. In the context of heterogeneous scenes, the ISRF can be altered due to non-uniform illumination and instabilities in the optical PSF. This leads to deformation in the ISRF with respect to the centroid, shape and the FWHM.

(Veefkind et al., 2012), launched in 2017, with the Tropospheric Monitoring Instrument (TROPOMI) being the single payload, Hu et al. (2016) showed that the stability and knowledge of the ISRF is the main driver of all instrument calibration errors for the retrieval accuracy. Landgraf et al. (2016) estimate the error of the retrieved CO data product due to non-uniform slit illumination to be in the order of 2 % with a quasi random characteristics. Noël et al. (2012) quantify the retrieval error for the upcoming Sentinel-4 UVN imaging spectrometer for the tropospheric O_3, NO_2, SO_2 and HCHO. They identify a difference in the retrieval error depending on the trace gas under observation. The largest error occurs for NO_2 with a mean error of 5 % and a maximum error of 50 %. They propose a software correction algorithm, which is based on a wavelength calibration scheme individually ~~to all Earthshine~~ applied to all Earth radiance spectra. As discussed by Caron et al. (2019), this type of software correction can only be applied to dedicated bands (~~UVN,UV-VIS~~UV,VIS,NIR) but is failing particularly in the SWIR absorption band due to the strong absorption ~~bands~~ lines of highly variable atmospheric components.

Sentinel-5/UVNS (Irizar et al., 2019) is the first push-broom spectrometer that employs an onboard concept to mitigate the effect of non-uniform scenes in the along-track direction. A hardware solution called slit homogenizer (SH) is implemented which reduces the scene contrast of the Earth radiance in the along track direction (ALT) of the satellite flight motion by replacing the classical slit with a pair of two parallel extended mirrors ~~in the along track direction (ALT) of the satellite flight motion (~~(Fig. 3a). The ~~distance between the~~ two parallel rectangular mirrors ~~is of $b = 240$ µm (NIR)~~composing the entrance slit have a distance of $b = 248$ µm, side lengths of 65 mm in ACT and a length of ~~9.6 mm~~ 9.91 mm (SWIR-3) along the optical

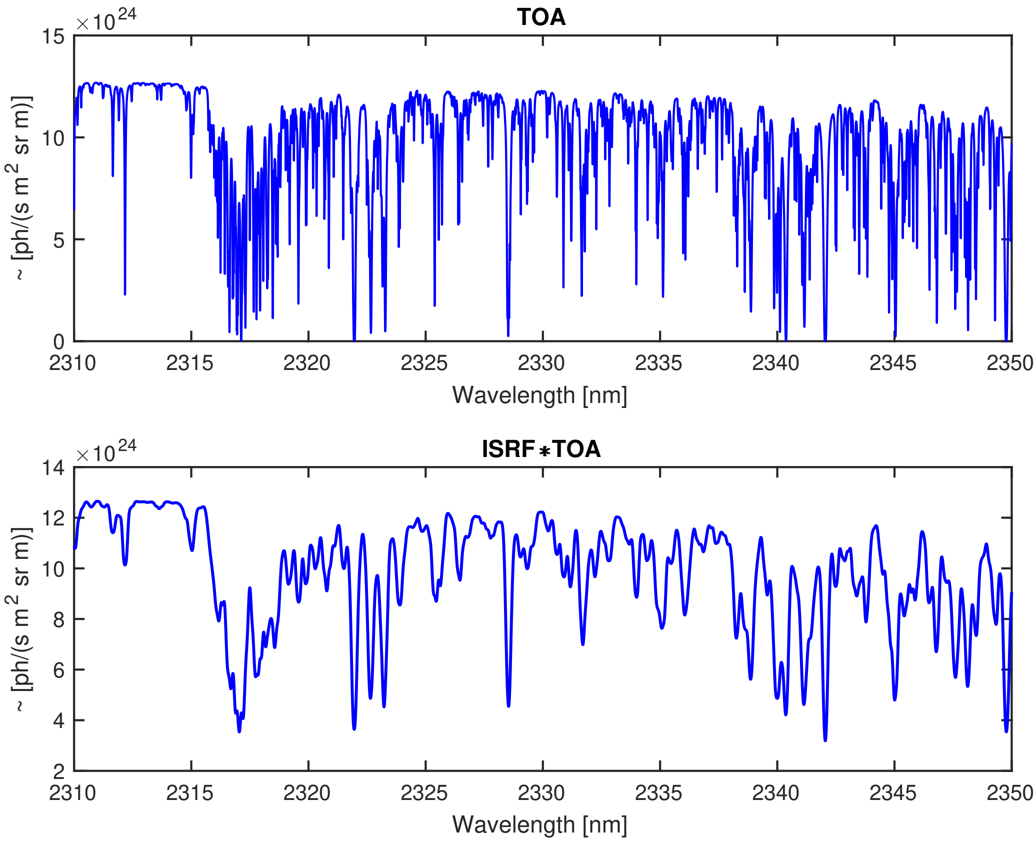

Figure 2. (Top) Representative high-resolution Earth Top-of-Atmosphere (TOA) spectrum ~~entering~~ incident on a space-borne instrument~~in the SWIR-3 wavelength band~~. The structures originate from the absorption features by CH_4, CO and H_2O. (Bottom) TOA spectrum convolved with a constant exemplary ISRF. Whenever the ISRF deviates from the the on-ground characterized shape, the measured spectrum, which sets the basis for the retrieval algorithms, will be altered.

axis. Thereby, the light focussed by the telescope optics onto the slit entrance plane ~~gets scrambled~~ is scrambled by multiple reflections in the ALT direction, whereas ~~the light in ACT~~ in ACT the light passes the SH without any reflection. Heterogeneous scenes in ACT direction may also affect the ISRF stability in the presence of spectrometer smile. This effect will not be covered in this study and instead we refer the reader to Gerilowski et al. (2011) and Caron et al. (2017). For a realistic reference Earth scene of the Sentinel-5/UVNS mission provided by ESA (~~S5-ESA-scene~~Fig. 5), the ~~total in orbit ISRF shape error budget is < 2 %, the~~ ISRF shall meet the requirements of < 2 % ISRF shape knowledge error, < 1 % relative Full width half Maximum (FWHM) ~~error < 1 % and the~~ knowledge error and 0.0125 nm centroid error in the ~~NIR 0.02 nm~~SWIR-3. Meister et al. (2017) and Caron et al. (2019) presented simulation results providing a first order ~~performance validation~~ prediction of the performance of the SH principle, which are relevant to achieve the performance requirements above. However, so far several second order effects haven't been quantitatively addressed in the ~~homogenization performance prediction~~ prediction of the homogenizing performance. This paper extents the existing first-order models and provides a more elaborated and comprehensive description of the SH and its impact on performance and instrument layout. We present an end-to-end model of the Sentinel-5/UVNS ~~NIR channel (760 nm~~SWIR-3 channel (2312 nm). In particular, we determine the spectrograph pupil illumination which is altered by the multiple reflections inside the SH. This effect changes the weighting of the aberrations present in the spectrograph optics and consequently ~~implies~~ results in a scene dependency in the optical PSF. As the ISRF is not only a function of the slit illumination, but also of the spectrograph PSF, a variation in the ~~spectrograph pupil intensity distribution~~ intensity distribution across the spectrograph pupil will ultimately put an uncertainty and error contribution to the ISRF. The severity of the spectrograph illumination distortion highly depends on the slit input illumination and the strength and type of aberrations present in the spectrograph. In order to quantify the achievable ISRF stability, we simulate several input scenes and different type of aberrations.

The outline of this paper is as follows: Sect. 2 describes the model we deployed to propagate the light through the SH by Huygens-Fresnel-diffraction formula. Applying Fourier optics, we formulate the propagation of the complex electric field from the SH exit plane up to the grating position, representing the reference plane for the evaluation of the spectrograph pupil intensity distribution. In ~~Section~~ Sect. 3 we quantify the spectrograph pupil intensity distribution for several Earth scene cases. The scene dependent weighting of the aberrations in the spectrograph and its impact on the ISRF properties is discussed and quantified in Sect. 4. Finally, we summarize our results in Sect. 5.

2 Slit Homogenizer Model

This section ~~contains details on~~ describes the underlying models and the working principle of the SH. The first part briefly summarizes the model developed by Meister et al. (2017), which ~~describes the field propagation~~ propagates the field through the Sentinel-5/UVNS instrument up to the SH exit plane by using a scalar-diffraction approach. ~~The second part focusses on the~~ In the second part a novel modelling technique of the spectrograph optics is introduced. We put a particular focus on the scene dependency of the spectrograph illumination while using a SH.

2.1 ~~Near Field~~Near-Field

The light from objects on the Earth, that are imaged at one spatial position (along slit) within the homogenizer entrance slit, arrive at the Sentinel-5/UVNS telescope entrance pupil as plane waves, where the incidence angle θ is between $\pm 0.1°$. The extent of the wavefront is limited by the size and shape of the telescope aperture. Neglecting geometrical optical aberrations, the telescope would create a diffraction limited point spread function ~~with the characteristic airy disc size~~ in the telescope image where the SH entrance ~~slit~~ plane is positioned. Depending on the angle of incidence, the PSF centroid will be located at a dedicated position within the ~~entrance slit. The characteristic airy disc in the entrance slit~~ SH entrance plane. The electric field of the diffraction pattern in the SH entrance plane is given as ~~(Goodman, 2005, p. 103)~~ the Fourier transform of the complex electric field over the telescope pupil. For a square entrance pupil, the diffraction pattern is calculated as: (Goodman, 2005, p.103)

$$\tilde{U}_{f,\theta}\left(u_a, v_a\right) = \frac{A}{i\lambda f} e^{-i\frac{k}{2f}\left(u^2+v^2\right) i\frac{k}{2f}\left(u_a^2+v_a^2\right)} \int\limits_{\Omega} e^{iky\ sin(\theta) iky_t\ sin(\theta)} e^{-i\frac{k}{f}(xu+yv)-i\frac{k}{f}(x_t u_a+y_t v_a)}\, dxdy du_a dv_a \tag{1}$$

$$= \frac{iAD^2}{\lambda f} e^{-i\frac{k}{2f}\left(u^2+v^2\right) i\frac{k}{2f}\left(u_a^2+v_a^2\right)} sinc\left(\frac{Dk}{2f} u_a\right)\ sinc\left(\frac{Dk}{2f}\left(f sin(\theta) - v_a\right)\right) \tag{2}$$

where ~~(x, y)~~ (x_t, y_t) are the coordinate positions in the telescope entrance pupil and ~~(u, v)~~ (u_a, v_a) are the respective coordinates in the SH entrance plane. Ω denotes the two-dimensional entrance pupil area, f is the focal length of the telescope, A the amplitude of the plane wavefront at the telescope entrance pupil, D the full side length of the quadratic telescope entrance pupil and $k = \frac{2\pi}{\lambda}$ the wavenumber. Further, the relation $\int_{-a}^{a} e^{ixc} = 2asinc(ca)$ and a Fresnel approximation was applied in Eq. (2). The propagation of $\tilde{U}_f$ through the subsequent SH is described by the Huygens-Fresnel principle (Goodman, 2005, p. 66). The reflections at the two mirrors are accounted for by inverting the propagation component in ALT upon every reflection n as

$$U_{f,\theta}(u_a, v_a) = R^{|n|} e^{in\pi} \tilde{U}_{f,\theta}\left(u_a, (-1)^n (v - nb v_a - nb)\right), \qquad \text{for } v_a \in \left[-\frac{b}{2} + nb, \frac{b}{2} + nb\right] \tag{3}$$

where R is the reflectivity, b is the slit width and $e^{in\pi}$ describes a phase jump upon every reflection n. Inserting Eq. (2) into (3) and applying the Huygens-Fresnel diffraction principle yields the expression for the intensity distribution at the SH exit plane for a given incidence angle θ, SH length l and position ~~$r(u, v) = \sqrt{l^2 + (x-u)^2 + (y-v)^2}$ as~~ $r(u_a, v_a) = \sqrt{l^2 + (u_b - u_a)^2 + (v_b - v_a)^2}$ as

$$U_\theta(u_b, v_b) = \frac{lAD^2}{\lambda^2 f} \int\limits_{u_a \in \mathbb{R}} \int\limits_{v_a = -\frac{b}{2}}^{v_a = \frac{b}{2}} \sum_{n \in \mathbb{N}} R^{|n|} \frac{e^{i\frac{k}{2f}\left(u_a^2 + ((-1)^n (v_a - nb))^2\right) + ikr(u_a, v_a + nb) + in\pi}}{r^2(u_a, v_a + nb)}$$
$$\cdot\, sinc\left(\frac{Dk}{2f} u_a\right) sinc\left(\frac{Dk}{2f}\left(f sin(\theta) - (-1)^n\ v_a\right)\right) du_a dv_a \tag{4}$$

where u_b, v_b are the coordinates of the position at the SH exit plane. Evaluating Eq. (4) for every incidence angle of the Sentinel-5/UVNS field of view (FoV) results in the so called SH transfer function (Fig. 3b), which maps any field point originating from Earth to an intensity distribution at the SH exit plane. In a purely geometric theory and a perfect SH configuration in terms of length, every point source would be distributed homogeneously in ALT direction (Fig. 3a). However, as is quantified in Eq. (4), the field distribution at the SH output plane highly depends on interference effects due to path differences of the reflected light inside the SH, resulting in a non-uniform transfer function as shown in Fig. ~~3a.~~ 3b.

A full experimental validation of the propagation model through the SH is still missing. An initial approach to validate the model in a breadboard activity was conducted by ITO Stuttgart and published in Irizar et al. (2019).

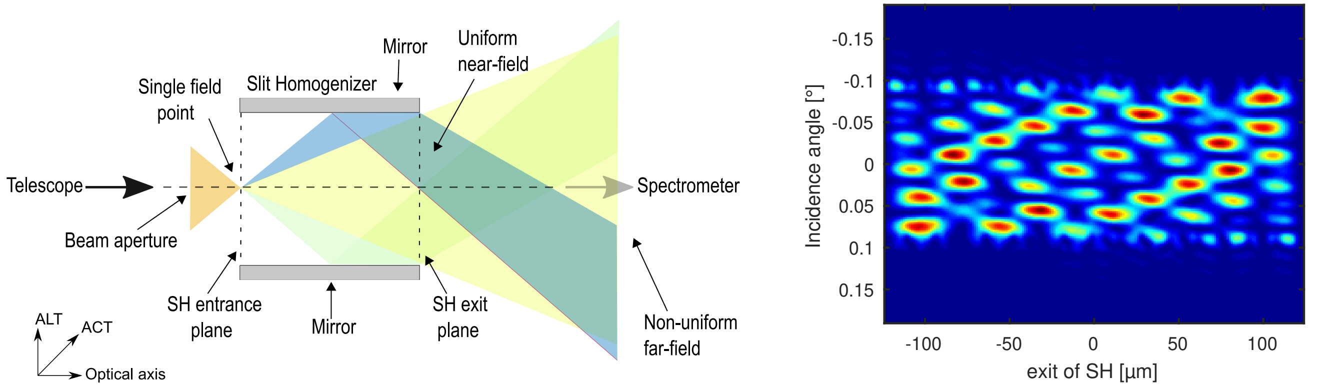

(a) Slit homogenization

(b) SH transfer function

Figure 3. (a) The SH homogenization principle based on a purely geometrical concept. With an appropriate length selection, the SH would perfectly homogenize any input scene. (b) SH transfer function. In reality, the output pattern of the SH is ~~highly dependent on~~ strongly affected by interference effects, resulting in a complex illumination pattern at the slit exit.

2.2 ~~Far Field~~Far-Field

In a space-based imaging spectrometer equipped with a classical slit acting as a field stop, a point source on the Earth surface enters the instrument as a plane wavefront with a uniform intensity over the telescope pupil. As this principle applies for every point source in a spatial sample on the Earth, the telescope pupil intensity homogeneity is independent of the radiance variation among the point sources in a spatial sample. Besides some diffraction edge effects in the slit plane, the telescope pupil intensity distribution gets retrieved in the spectrograph pupil. This is not the case when introducing a mirror based SH. Existing SH models (Meister et al. (2017) and Caron et al. (2019)) implement the spectrometer as a simple scaling factor and the ISRF on the FPA is obtained via the convolution of the SH output intensity distribution, the pixel response implemented as a characteristic function and the spectrograph PSF. In this contribution we model the propagation through the spectrograph more accurately by including the spectrograph optics, such as the collimator, a dispersive element and the imaging optics. In particular, the inclusion of these optical parts becomes important because the SH not only homogenizes the scene contrast in the slit, but it also significantly modifies the spectrograph pupil illumination. A schematic diagram of the SH behaviour and the instrument setup is shown in Fig. 4. A plane wavefront with incidence angle Θ is focussed by a telescope on the SH entrance ~~pupil~~plane. In ACT direction, the light is not affected by the SH. After a distance l, corresponding to the SH length, the diffraction limited PSF at the SH entrance ~~pupil~~ plane is converted to the ~~far field~~ far-field pattern of the diffraction ~~limited airy-disc~~pattern. Independent of the applied scene in ACT, the telescope pupil ~~is~~ intensity distribution in ACT is mostly retrieved again at the spectrograph pupil~~despite a~~. The exact distribution of the spectrograph pupil illumination is affected by magnification factor and a truncation of the electric field at the SH entrance plane, which leads to a slight broadening and small intensity variations with a high frequency in angular space (Berlich and Harnisch, 2017). In ALT the ~~light airy-disc~~ diffraction pattern in the SH entrance plane undergoes multiple reflections on the mirrors, so that eventually the whole exit plane of the SH

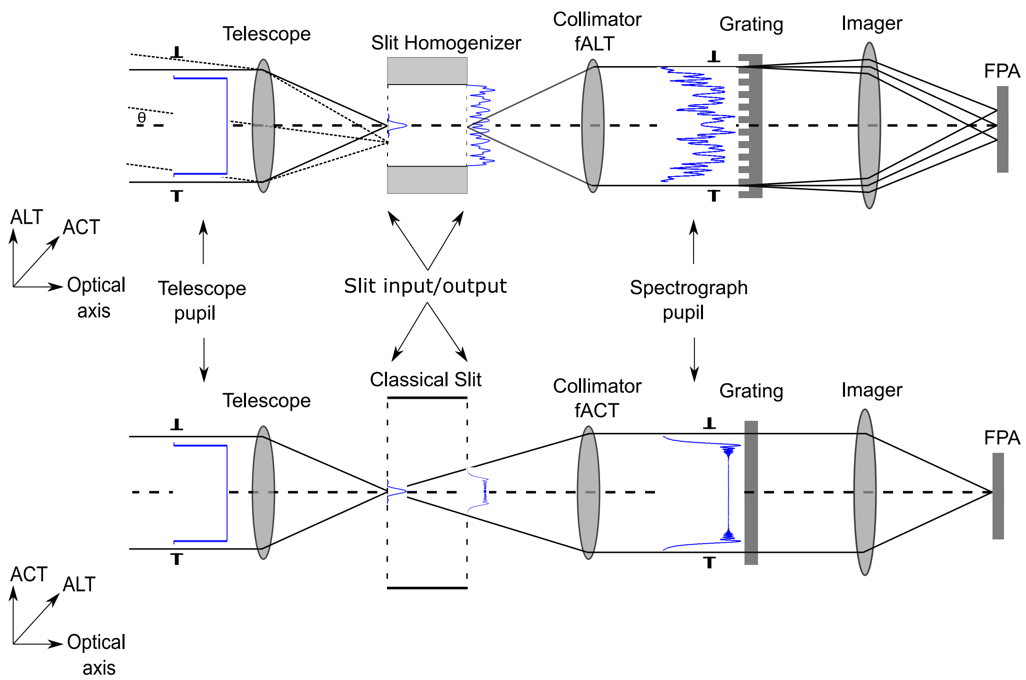

Figure 4. Generic setup of the SH in the Sentinel-5/UVNS instrument. A plane wavefront gets focussed in the SH entrance plane and the propagation of such stimulus is shown in blue as the square modulus of the electric field. The incoming light undergoes several reflections in ALT direction, whereas the SH in ACT is similar to a classical slit acting as a field stop. The ~~slit~~ collimator contains an astigmatic correction which is adjusted to the slit length. The SH homogenizes the scene in ALT direction but also modifies the spectrograph pupil illumination. The grating ~~is a 1D binary phase grating which~~ disperses the light in ALT. The pupil distribution in ACT direction is conserved except for diffraction effects due to truncation of the telescope PSF in the slit plane.

is illuminated. ~~Hence, the object plane is defocused by the SH length~~To preserve the full image information along the swath, the entrance plane of the SH must be imaged; to homogenize the scene in ALT the exit plane of the SH must be imaged. This is achieved by an astigmatism in the collimator optics. Moreover, the multiple reflections inside the SH lead to a modification of the system exit pupil illumination. In other words, the SH output plane (~~near field~~near-field) and the spectrograph pupil intensity variation (~~SH far field~~far-field) strongly depend on the initial position of the incoming plane wave, and therefore on the Earth scene radiance in ALT direction. Following a first simple geometrical argument as discussed by (Caron et al., 2019), we consider a point source at the SH entrance. The rays inside the cone emerging from this source will undergo a number of reflections depending on the position of the point source and the angle of the specific ray inside the cone. The maximum angle is given by the telescope F-Number. With this geometrical reasoning it becomes obvious, that the number of reflections differs among the rays inside the cone. If the number of reflections is even, a ray keeps its nominal pupil position; whereas if the number is odd, its pupil coordinate will be inverted. From this argument we deduce that the spectrograph pupil illumination will be altered with respect to the telescope pupil ~~. In the~~ illumination. Note, that the reallocation of the angular distribution of the light has a different origin, than the remaining inhomogeneity at the SH exit plane. The achieved near-field homogenization is dependent on the remaining interference fluctuations in the SH transfer function. In contrast, the variations in the spectrograph illumination is based on a geometrical reallocation of the angular distribution of the light exiting the SH in combination with interference effects in the spectrograph pupil plane.

In the following we make ~~this~~ the geometrical argument rigorous using diffraction theory. A general case for the connection between slit exit plane and spectrograph pupil plane is considered by Goodman (2005, p. 104). In the scenario discussed there, a collimated input field ~~$U_l(x,y)$~~ $U_l(x_s,y_s)$ propagates through a perfect thin lens at a distance d. The field in the focal plane of the lens is then given by:

$$U_f(u_b,v_b) = \cancel{\frac{A}{i\lambda f}}\frac{1}{i\lambda f}\, exp\left(i\frac{k}{2f}\left(1-\frac{d}{f}\right)\left({u_b}^2+{v_b}^2\right)\right)\int\limits_{-\infty}^{\infty}\int\limits_{-\infty}^{\infty} U_l(x_s,y_s)\, exp\left(-i\cancel{\frac{2\pi}{\lambda f}}\frac{k}{f}\left(\cancel{xu}x_s u_b+\cancel{yu}y_s v_b\right)\right)\cancel{dxdy}dx_s dy_s \tag{5}$$

where ~~k is the wavevector of the incoming wave, λ is the wavelength and f is the focal length of the lens. Hence~~ x_s, y_s are the position in the spectrometer pupil plane and u_b, v_b the coordinates in the image plane at the SH exit. Indeed, the field at the lens focal plane is proportional to the two-dimensional Fourier transform.

In contrast, our situation is inverted as we are interested in ~~$U_l(x,y)$~~ $U_l(x_s,y_s)$, i.e. the collimated field distribution ~~after the collimation optics~~ at the spectrometer pupil originating from the SH output plane. ~~By using Fourier theory and applying $d = f_{col,ALT}$ we obtain the field distribution at the position of the diffracting gratingas:~~ Further, we need to incorporate the astigmatism in the collimation optics and the diffraction grating. These steps are covered in the following two sections.

$$\cancel{U_l\left(\frac{2\pi}{\lambda f}x,\frac{2\pi}{\lambda f}y\right)=\frac{i}{A\lambda f}\int\int\limits_{-\infty}^{\infty}\int\limits_{-\infty}^{\infty}U_f(u,v)(u^2+v^2)\, exp\left(-i\frac{2\pi}{\lambda f}(xu+yv)\right)dudv}$$

2.3 Collimator astigmatism

~~The multiple reflections inside the SH in the ALT-dimension induces an anamorphism which means, that we get different object planes in ALT and ACT direction. The separation between the focal points corresponds exactly to the length of the SH . This is compensated by an astigmatismintroduced on the collimation optics~~In order to keep the full image information in ACT while imaging the homogenized SH output image, the collimator needs an astigmatism. In our model, this is implemented via Zernike polynomial terms on the collimation lens. We follow the OSA/ANSI convention for the definitions of the Zernike polynomials and the indexing of the Zernike modes (Thibos et al., 2000). ~~For the~~ The focal length of the ~~collimation optics we match the object plane in ALT direction, which corresponds to~~ collimator in ALT is such to image the SH exit plane~~. The first contribution to the Zernike term is a defocus with an appropriate coefficient, which shifts the object position from the SH exit plane to the centre of the SH. From there, we apply an astigmatism, which splits up the object plane into a sagittal focus corresponding to the telescope focus in ACT (SH input plane) and a tangential focus corresponding to the focus position in~~

~~ALT (SH exit plane) .~~, while in ACT the SH entrance plane is imaged. In the simulation this is realised with three terms: a focal length term where the focal length is that of the collimator in ALT, a defocus term to shift the object plane and an astigmatism term to separate the ALT (tangential) and ACT (saggital) object planes.

The Zernike polynomials are given by:

$$\text{Defocus:} \quad Z_n^m(\rho,\theta) = Z_2^0(\rho,\theta) = c_{02}\sqrt{3}(2\rho^2 - 1) \tag{6}$$

$$\text{Astigmatism:} \quad Z_n^m(\rho,\theta) = Z_2^2(\rho,\theta) = c_{22}\sqrt{6}\rho^2 sin(2\theta) \tag{7}$$

where ~~c is~~ c_{nm} are the Zernike coefficients, defining the strength of the aberration and Z_n^m the Zernike polynomials. Due to the elegant and orthonormal definition of the Zernike polynomials, a perfect matching of Defocus and Astigmatism amplitude is ~~straight forward~~straightforward, as the difference between the sagitta and tangential plane of the astigmatism is solely dependent on the radial term of the Zernike polynomial. Therefore, in order to match the corresponding difference given by the SH length, the weighting of the astigmatism has to be larger than the defocus term by a factor of $\sqrt{2}$~~, which can be derived by comparing the prefactor of the radial terms in~~ $\cancel{Z_n^m}$ ~~of Defocus and Astigmatism~~. Hence, the combined Zernike term will be:

$$H(\rho,\theta) = c\, Z_2^0(\rho,\theta) + \sqrt{2}\, c\, Z_2^2(\rho,\theta) \tag{8}$$

Including the ~~astigmatic correction~~ astigmatism of the collimation optics~~in the wavefront propagation modifies equation ?? into:~~, applying $d = f_{col,ALT}$ and solving eq. (5) for $U_{l,\theta}$ by using the coordinate transformation $x'_s = \frac{k}{f}x_s$ and $y'_s = \frac{k}{f}y_s$, we get the field distribution at the diffraction grating as:

$$U_{l,\theta}\left(x'_s, y'_s\right) = \frac{i}{\lambda f} e^{ik\left(c\ Z_2^0(\rho,\theta) + \sqrt{2}\ c\ Z_2^2(\rho,\theta)\right)} \cdot \int\limits_{-\infty}^{\infty}\int\limits_{-\infty}^{\infty} U_{f,\theta}(u_b, v_b)\ \ exp\left(i\frac{k}{f}(x'_s u_b + y'_s v_b)\right) du_b dv_b \tag{9}$$

Equation 9 yields the field distribution incident on the diffraction grating. The implementation of the diffraction grating, which is responsible for the wavelength dispersion will be introduced in the next section.

2.4 Diffraction grating

The primary goal of the spectrometer is to distinguish the intensity of the light as a function of the wavelength and spatial position. In order to separate the wavelengths a diffractive element is placed in the spectrograph pupil and disperses the light in the ALT direction. For our analysis, we place the diffraction grating at a distance $d = f_{col,ALT}$ after the collimator and on the optical axes. Further, we model the dispersive element as a 1D binary phase diffraction grating. Such gratings induce a π phase variation by thickness changes of the grating medium. Three design parameters are used to describe the grating and are unique for every spectrometer channel: the period of the grating Λ, the phase difference Φ between the ridge (of width d) ~~,~~ and the groove regions of the grating, and the fill factor d/Λ. Physically, the phase difference itself is induced by two parameters: the height or thickness t of the ridge and the refractive index of the material of which the grating is made. In most cases, the refractive index of the used material is fixed and the thickness of the material is the primary parameter. The phase profile with a fill factor of 0.5 which provides the maximum efficiency in ALT direction is given by:

$$\Phi_{1D}\left(y_s\right) = \begin{cases} \pi & 0 \leq y_s \bmod \Lambda \leq \frac{\Lambda}{2} \\ 0 & \frac{\Lambda}{2} \leq y_s \bmod \Lambda \leq \Lambda \end{cases} \tag{10}$$

The complex electric field of the spectrograph pupil wavefront after the diffraction grating is then given by:

$$U_{\cancel{g}g,\theta}(x'_s,y'_s) = U_{\cancel{l}l,\theta}(x'_s,y'_s)\ e^{\cancel{i\Phi(y)}i\Phi(y_s)} \tag{11}$$

The intensity distribution after the grating is given by inserting equation (9) in (11) and applying the absolute square:

$$I_{\cancel{g}g,\theta}(x'_s,y'_s) = |U_{\cancel{g}g,\theta}(x'_s,y'_s)|\cancel{.}^2 \tag{12}$$

The implementation of the diffraction grating is a simplified model, which is an approximation of the real, more complex case. In Sentinel-5/UVNS, the SWIR spectrograph is equipped with a silicon immersed grating. The simplified approach is valid, as the SH does not affect the general behaviour of the grating.

3 Spectrograph pupil intensity distribution

The ~~far field~~ far-field intensity distribution is ~~highly~~ dependent on the contrast of the Earth scene in ALT and therefore on the SH entrance ~~illumination. In order to~~ plane illumination. We characterize the amplitude of the ~~spectrograph pupil intensity distribution, we introduce several Earth scene cases and therefore slit illuminations in ALT as depicted in Fig 5. The test cases contain a uniform scene, a representative Earth scene~~ variations of the spectrograph pupil illumination by introducing two types of heterogeneous scenes. First, an applicable Earth scene as defined by ESA for the Sentinel-5/UVNS ~~instrument provided by ESA (S5-ESA-scene) and stationary high contrast calibration scenes, which corresponds to the case~~mission, which aims at representing a realistic Earth scene case. The on ground albedo variations of this scenes can be parametrized as a linear interpolation between two spectra, representing the same atmospheric state, but obtained with either a dark or bright albedo (Caron et al., 2017). The spatial variation of the scene heterogeneity is described by introducing interpolation weights w_k. The resulting spectrum for a given ALT subsample k is then calculated as:

$$L_k\left(\lambda\right) = \left(1 - w_k\right)\ L_{dark}\left(\lambda\right) + w_k\ L_{bright}\left(\lambda\right) \tag{13}$$

where the ~~SH ALT entrance plane is partially illuminated by 75 %, 50 % and 25 %. Further, we also show the spectrograph pupil for a single point source at the SH entrance. Fig. 5 shows the top of atmosphere (ToA) radiance level given by a realistic Earth scene for the~~ reference spectra correspond to a Tropical bright scene (L_{bright} - albedo = 0.65) and a Tropical dark scene (L_{dark} - albedo = 0.05). The weighting factors that were used for this study have been derived from the Moderate

Resolution Imaging Spectroradiometer (MODIS) surface reflectance products with 500 m spatial resolution and total coverage of 25 km for relevant conditions of Sentinel-5/UVNS ~~instrument. Due to smearing of the satellite's movement , this scene has a significantly lower contrast than the calibration scenes. Here we want to emphasize that future missions depending on their spatial and spectral resolution as well as their desired data product may have even more stringent requirements on the scene homogeneity. The~~ $\cancel{CO_2}$ ~~Monitoring Mission (CO2M) aims to detect strong, almost point like~~ $\cancel{CO_2}$ ~~and~~ $\cancel{CH_4}$ ~~emission sources with a spatial resolution of~~ $\cancel{4\ \mathrm{km}^2}$ ~~(Sierk et al., 2019). In order to achieve a maximum error of~~ $\cancel{XCO_2}$ ~~of~~ $\cancel{0.5\ \mathrm{ppm}}$~~, an ISRF shape stability of~~ $\cancel{< 1.5\ \%}$ ~~over a maximum contrast scene is required. This corresponds to a sharp transition from bright to dark slit illumination as shown for the calibration scenes in Fig. 5.~~

(EOP PIO, 2011). The slit smearing due to platform movement is accounted for by convolving the on ground scene with the motion boxcar of the spatial sampling distance (SSD). The platform movement is acting like a low-pass filter and averages out short albedo variations with respect to the SSD and the instruments FoV. However, without a SH, remaining inhomogeneities are present in the slit which yield up to $20\ \%$ slit illumination variations in ALT directions. Figure 5 depicts the on ground albedo contrast given in terms of weighting factors w_k, the scene after smearing due to the motion of the platform and the location of the SH entrance plane. We assume the scene to be homogeneous in ACT direction. In fact, heterogeneous scenes in ACT direction may also affect the ISRF stability in the presence of spectrometer smile (see Gerilowski et al. (2011) and Caron et al. (2017)).

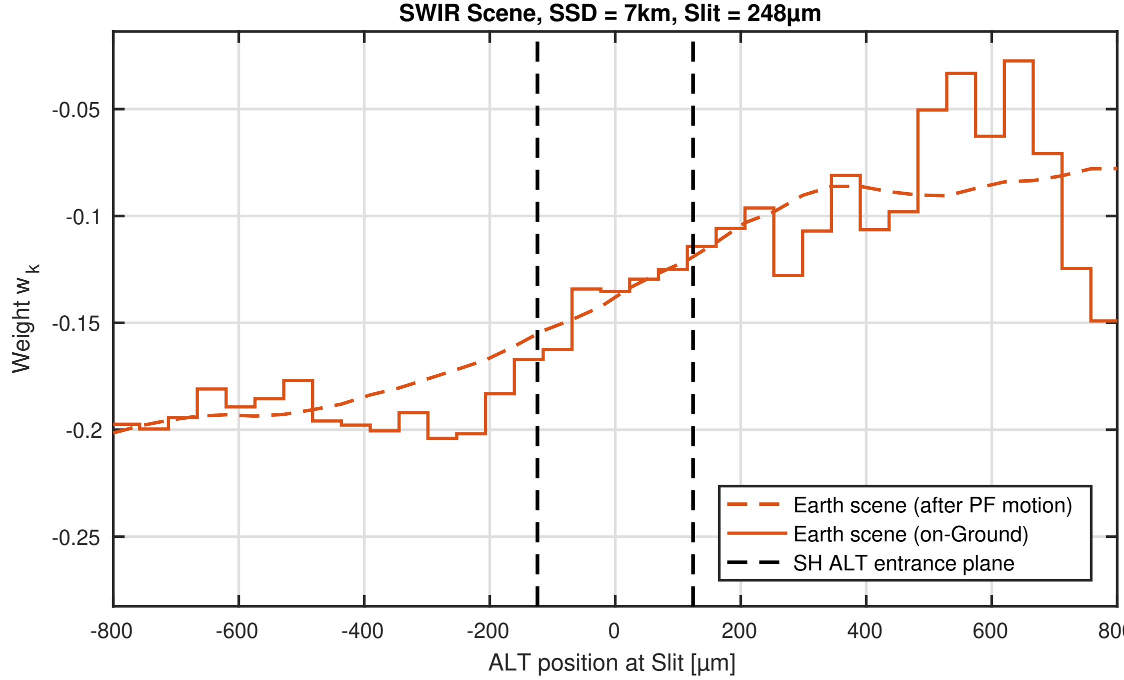

Figure 5. ~~Applied input Earth scenes~~ Realistic Earth scenes in the SWIR-3 derived from MODIS images corresponding to the slit illumination in ALT. ~~This includes a representative scene for the Sentinel-5/UVNS instrument and several high contrast calibration scenes with 75%, 50% and 25% slit illumination.~~ The on ground surface albedo is given in terms of weight factors w_k in the solid line. The same scene after smearing with a boxcar of the spatial sampling distance (SSD) accounting for the platform motion is given in the dashed line. The scene contrast including the platform motion in the plane of the SH entrance plane will be the reference scene for this study.

The second scene considered represents an artificial calibration (CAL) scene where 50 % of the slit is illuminated and 50 % is dark. These kind of instantaneous transitions are impossible to be observed by a push-broom instrument with finite FoV and integration time. However, they are convenient to be applied in experimental measurements and will serve as reference to experimentally validate the SH performance models.

Figure 6 depicts the simulation results for the pupil intensity distribution in the ~~NIR (760 nm~~ SWIR-3 (2312 nm) for the applied test scenes as well as a homogeneous slit illumination. As expected, the uniformity of the input telescope pupil illumination is completely conserved in ACT direction ~~as no~~ due to the absence of interaction, i.e. reflection, with the SH ~~is happening~~. Therefore the top-hat intensity distribution of the telescope is, besides diffraction edge effects, completely ~~retrieved. Contrary~~ preserved. To the contrary, the intensity distribution in ALT is ~~highly~~ dependent on the contrast of the applied scene. Even for a homogeneous scene the SH modifies the pupil intensity (Fig. 6a) and consists of symmetrical variations. The intensity pattern just varies slightly for the ~~S5-ESA-Scene~~ applicable Earth scene (Fig. 6b) due to the ~~low contrast in the scene. However, for high contrast calibration~~ moderate gradient of the slit illumination variation. The CAL scenes (Fig. 6 c,d~~,e) the~~

~~SH drastically disturbs the uniformity of the spectrograph pupil , leading to a maximum of 80 % peak to valley intensity modulation (c).~~

) highlight the previously made geometrical argument for the non-uniform pupil illumination as parts of the pupil are left with only a fraction of the light. For illustration, we show a case where the upper 50 % of the slit are illuminated and another case where the lower 50 % of the slit are illuminated (representing the ALT illumination).

In the next section we will investigate the impact of non-uniform pupil illumination in combination with spectrograph aberrations on the ISRF stability.

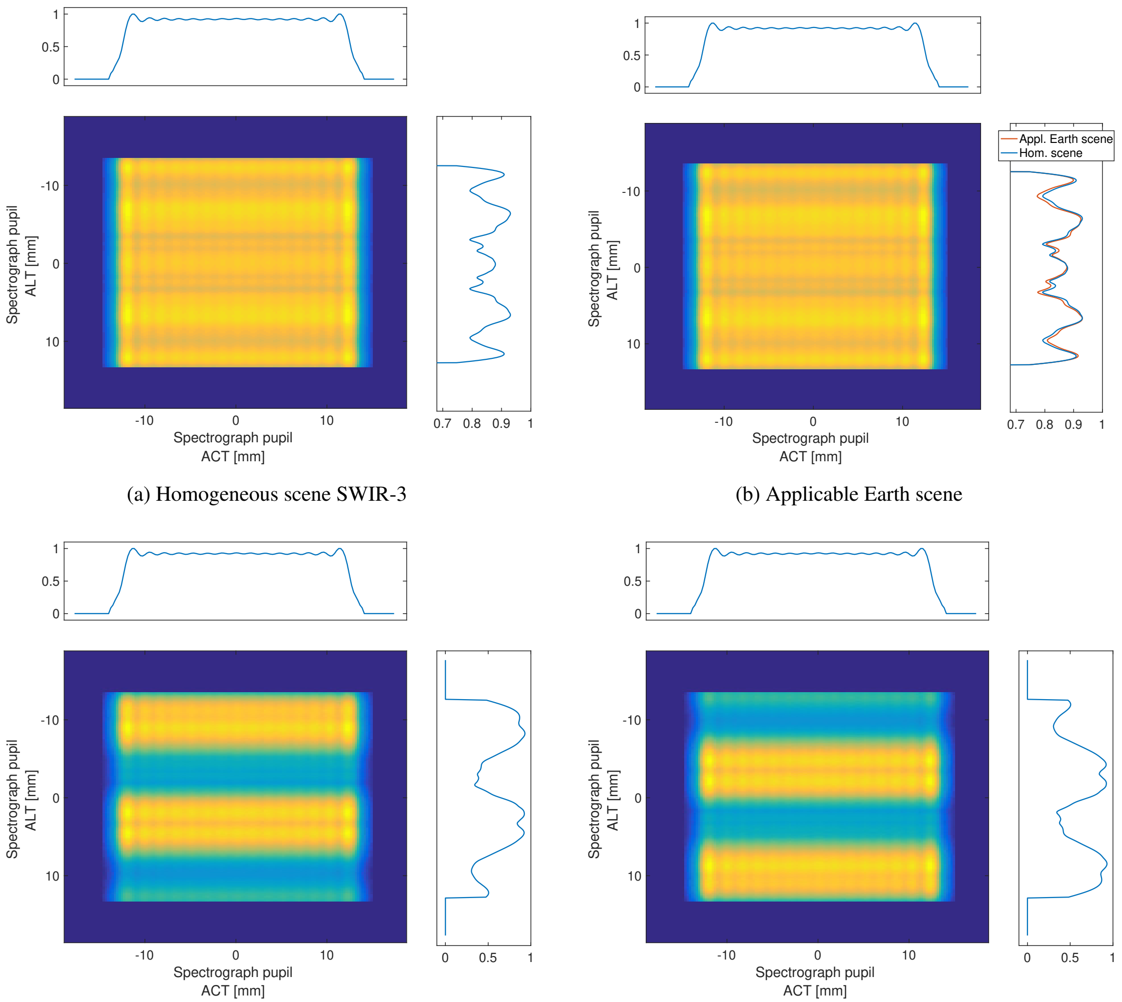

(a) Homogeneous scene SWIR-3

(b) Applicable Earth scene

(c) 50 % CAL scene - bottom

(d) 50 % CAL scene - top

Figure 6. ~~Spectrograph~~ Simulation results of the spectrograph pupil intensity distribution in the ~~NIR~~ SWIR-3 (~~760 nm~~2312 nm) for different slit illuminations. The uniformity of the pupil in ALT is ~~highly~~ dependent on the applied scene. ~~As expected the~~ The ACT uniformity from the telescope pupil is ~~conserved~~ preserved, as there is no interaction with the SH.

4 Impact on ISRF

The main impact of the above described variations in the spectrometer pupil illumination is the scene dependent weighting of the aberrations inherent to the spectrograph optics. In ~~a simplified view,~~ the case of a classical slit, it is valid to calculate the ISRF of an imaging spectrometer ~~is given by~~ as the convolution of the slit illumination, the pixel response on the FPA and the optical PSF of the spectrograph optics. ~~A~~ When using a SH, a scene dependency of the spectrograph pupil illumination will weight the aberrations of the system accordingly and thereby create ~~an error~~ a variation in the PSF, which will ultimately also ~~affect~~ change the ISRF properties.

~~Instead of~~ Therefore, it is necessary to keep the complex phase of the electric field during the propagation through the instrument.

Instead of a convolution, we propagate the spectrograph pupil illumination through the imaging optics by diffraction integrals. For the description of the aberrations present in the Sentinel-5/UVNS instrument we use again the formulation of Zernike theory. We know from ray tracing simulation predictions the PSF size on the FPA of the Sentinel-5/UVNS ~~NIR~~ SWIR-3 channel, which in ~~a simplified model is given~~ the case of a classical slit can be approximated by the standard deviation of a normal distribution. ~~As the actual aberrationspresent in the system are yet unknown~~In order to assess the impact of aberrations, we impinge different types of aberrations on the spectrograph imaging optics and match the PSF size to the ~~design~~ instrument prediction. As the shape of the PSF for an arbitrary aberration is not given by a normal distribution, we define the PSF size as the area where 80 % of the encircled energy (EE) is contained. Then we tune the strength of the aberration coefficients in such a way that the size of the aberrated PSF matches ~~the case where we assume a normal distribution as~~ that of the normal distributed PSF. For the transformation of the spectrograph pupil illumination to the FPA including aberrations, we apply the thin lens formula and expand it by adding the phase term for the Zernike aberrations (Goodman, 2005, p. 145). Our starting point for the propagation is the grating position where, for the case of Sentinel-5/UVNS, the distance d is matching the focal length of the imaging optics. In that case the formulation simplifies again and is given by a relation which has the form of a Fourier transform:

$$U_{FPAFPA,\theta}(us, vt) = \frac{2\pi}{i\lambda f_{im}} \frac{1}{i\lambda f_{im}} \int\limits_{-\infty}^{\infty} \int\limits_{-\infty}^{\infty} U_{gg,\theta}(x'_s, y'_s)\, exp\left(-i \frac{2\pi}{\lambda f_{im}} \frac{k}{f_{im}} \left(xux_s s + yuy_s t\right)\right) exp\left(\frac{-ik}{\pi} \frac{ik}{\pi} H(r,\phi)\right) dxdydx_s dy_s \tag{14}$$

where s, t are the coordinates at the FPA, f_{im} is the focal length of the imager, ~~U_g~~ $U_{g,\theta}$ the field distribution at the grating and $H(r,\phi)$, with ~~$r = r(x,y)$ and $\phi = \phi(x,y)$~~ $r = r(x_s, y_s)$ and $\phi = \phi(x_s, y_s)$, the respective Zernike aberration that we apply. Any spatially incoherent monochromatic input scene can be distributed in plane wavefronts with amplitude $A(\Theta)$. Each such wavefront leads to an intensity ~~$I = I_\Theta(u,v) = |U_{FPA}|^2$~~ $I = I_\Theta(s,t) = |U_{FPA,\theta}|^2$ on the FPA. As we have no SH impact in ACT direction, we collapse this dimension and sum along it. This yields the ~~$1D$~~ 1D ISRF intensity distribution on the FPA as a function of the incidence angle Θ as ~~$I_\Theta(v)$~~ $I_\Theta(t)$. The respective scene will weight the intensities on the FPA depending of their strength and is therefore the linear operator:

$$I_{vt} = \int_{\Theta\in\mathcal{R}\Theta\in\mathbb{R}} A(\Theta) I(\Theta, vt)\, d\Theta = I \circ A(vt) \tag{15}$$

Note that for a homogeneous scene, $A(\Theta) = 1$ for every incidence angle. Finally, the normalized ISRF on the FPA is given by:

$$\widetilde{ISRF}(vt) = ((I_\Theta \circ A) * \chi * N_\sigma(vt) \tag{16}$$

$$ISRF(vt) = \frac{\widetilde{ISRF}(v)}{\alpha \int \widetilde{ISRF}(v) dv} \frac{\widetilde{ISRF}(\frac{t}{\alpha})}{\alpha \int \widetilde{ISRF}(t)\, dt} \tag{17}$$

where χ is the characteristic function, which is 1 inside a pixel area and 0 elsewhere, α a scaling factor to give the ISRF in units of wavelength and N_σ is the density function of a normal distribution with zero mean value and standard deviation σ. The latter factor accounts for the modulation transfer function (MTF) of the detector (not the MTF of the whole optical system). In order to asses the stability of the ISRF we define three merit functions:

– Shape error, which we define as the maximum difference of the ISRF calculated for a homogeneous and heterogeneous scene respectively

$$\text{Shape error} := \max_{vt} \left| \frac{ISRF_{hom}(v) - ISRF_{het}(v)}{\max_{\tilde{v}} ISRF_{hom}(\tilde{v})} \frac{ISRF_{hom}(t) - ISRF_{het}(t)}{\max_{\tilde{t}} ISRF_{hom}(\tilde{t})} \right| \tag{18}$$

– Centroid error: Shift of the position of the spectral channel centroid, where the centroid is defined as

$$\text{CentroidCentroid error} := \frac{\int_{FPA} ISRF(v)\, v\, dv}{\int_{FPA} ISRF(v)} \frac{\int_{FPA} ISRF(t)\, t\, dt}{\int_{FPA} ISRF(t)} \tag{19}$$

– ~~Spot size~~ Spectral resolution of the ISRF given by the FWHM

~~For our~~ We consider two cases for the assessment of the induced ~~change in ISRF stability, we distinguish three different cases of calculation. First, we calculate the ISRF merit functions (Shape, centroid, FWHM) for the case, where the PSF is given by a normal distribution simply~~ impact on the ISRF stability. In the first case, we neglect any variation of the spectrograph illumination and use the PSF as a convolution kernel of the ISRF given as a constant and scene independent normal distribution defined as:

$$g(vt) = \frac{1}{\sigma\sqrt{2\pi}}\, exp\left(-\frac{v^2}{2\sigma^2}\frac{t^2}{2\sigma^2}\right) \tag{20}$$

where σ is the standard deviation representing the size of the PSF~~(e. g. 19.1 μm in NIR~~ [1] . The spot size value for a representative field point ~~). In that case~~in the SWIR-3 spectrometer of Sentinel-5/UVNS is about 6.85 μm. When convolving

[1] ~~Preliminary analytical value~~

with a gaussian PSF, we neglect the non uniformity in the pupil and the spectrometer aberrations and the ISRF errors are only driven by the slit exit illumination (near-field). For the second case, we impinge a certain amount of ~~pure spherical~~ aberrations on the imaging optics to get the same spot size for the PSF as in the first case. In this case, the ISRF errors are a combination of the remaining inhomogeneities at the SH exit plane (near-field), as well as effects due to non-uniform spectrograph illumination (far-field). The aberrations present in the Sentinel-5/UVNS spectrograph are dependent on the position on the FPA in spectral and spatial direction. In the upcoming characterization and calibration campaign, the specific types of aberration of the final instrument will not be determined, but only the size of the spots. Therefore, although not a realistic case~~1. Spherical aberrations are radially symmetric like the Airy pattern itself and the size of the central bright spot does not change with increasing amount of spherical aberrations. As a third case~~, we ~~apply pure comatic aberrations , which behave fundamentally different than spherical aberrations and have radial and azimuthal contributions in the phase map. The wavefront errors induced by comatic aberrationshave reverse symmetry along the axis of aberration, with one side flatter and the other more curved~~ impinge pure aberrations of a single type in order to determine critical Zernike terms for the ISRF stability. We also test two mixtures of different types of aberrations, which represent more realistic field points of Sentinel-5/UVNS. The ISRF for a homogeneous scene including aberrations, will be extensively characterized on-ground. We want to investigate how the ISRF based on several Zernike terms behave under the condition of non-uniform scenes and how the ISRF deviation evolves with respect to ~~its perfect reference wavefront. Their formulation in Zernike polynomials is given by:~~

$$\text{Spherical Aberration}: \quad Z_n^m(\rho,\theta) = Z_4^0(\rho,\theta) = c\sqrt{5}(6\rho^4 - 6\rho^2 + 1)$$

$$\text{Vertical Coma}: \quad Z_n^m(\rho,\theta) = Z_3^{-1}(\rho,\theta) = c\sqrt{8}(\rho^3 - 2\rho)sin(\theta)$$

each, aberration type specific, homogeneous ISRF. Therefore, in the next paragraph, we calculate the relative change in the ISRF figures of merit functions.

~~Clearly, a scene dependent mixture of the aberration weighting will create different result for the properties of the subsequently calculated ISRF . As the spectrograph pupil homogeneity, similar to the SH exit plane, is highly dependent on the scene that we apply, we calculate the ISRF properties for the scenes defined in Fig. 5. As a direct comparison of~~

5 Results and discussion

In the following, we present the ISRF figures of merit resulting from the simulation of several Zernike polynomials for the Sentinel-5/UVNS applicable heterogeneous Earth scene and a 50 % stationary calibration scene. Further, we compare the ~~difference between an ISRF calculated with a PSF disturbed by aberrations and a PSF given as a pure normal distribution is problematic, we rather compare the errors relative to a homogeneous scene .Table (??-??) summarizes the result of our calculations. It shows~~ results to the case of a classical slit without scene homogenization. Table 1 & 2 summarize the results for the ISRF figures of merit. Note that the errors for the ~~ISRF merit functions~~calibration scene are much larger than the errors for a realistic Earth scene. The calibration scene can be used in a laboratory to characterize the SH performance and compare it with the prediction. All Zernike polynomials increase the error in the ISRF knowledge compared to the case, where the ~~PSF is calculated with a normal distribution (??) , pure spherical aberrations (??) and comatic aberrations (??) for different SH input scenes. As expected, the absolute error goes up for every case as we apply higher scenecontrasts. In first order, this comes from the lacking capability of the SH to reduce very high scene contrasts and thereby the slit imaged on the detector has still prominent remnants of the scene contrast at the SH entrance plane. However as a secondary effect, we see that the strength of the errors is also critically dependent on the PSF specified by the aberrations that we apply and their respective weighting by the pupil intensity distribution.As expected, radially symmetric aberrations have no impact on the centroid and shape error but induce a higher FWHM error. Even for a scene with limited contrast as the S5-ESA-scene the FWHM error goes up by~~ ISRF is calculated as the convolution with a constant gaussian PSF. The error magnitude variation ranges from only small increasing errors (Defocus, Vertical astigmatism) to a notable increase of the error (Oblique quadrafoil, Horizontal Coma). The aberrations change both the maximum amplitude of the errors and the specific shape of the ISRF. Figure 7b depicts the ISRF assuming pure vertical coma, pure spherical aberrations and pure oblique trefoil for a heterogeneous 50 % calibration scene. The lower part of the plot shows the ISRF shape difference for each specific homogeneous reference scene. Note, that the shape error is defined as the maximum amplitude of the difference plot. As none of the field points in the real Sentinel-5/UVNS instrument will contain a pure singular type of aberration, we tested two set of aberration mixtures, which is more representative of a real field point in the Sentinel-5/UVNS instrument. Although our study doesn't provide a rigorous mathematical argument, the results indicate, that the error of the combined Zernike polynomials lies within the errors of the individual contributors. This argument is supported by Fig. 8, where we plotted the ISRF shape error, going from a pure oblique quadrafoil aberration to a pure defocus aberration. In each step we reduced the fraction of the quadrafoil aberration by 20 % and tuned the defocus aberration coefficient in such a way, that we ended up with the same PSF size of 6.85 μm (80 % EE). The ISRF errors always remain in the corridor between the case of pure oblique quadrafoil and pure defocus aberration. This behaviour was tested for several other Zernike combinations. From that we conclude, that the errors given in Table 1 & 2 for the respective Zernike polynomials span the error space, where mixtures of aberrations lie within.

Although the phenomena of the variations of the pupil illumination in combination with spectrometer aberrations increases the errors, the SH still homogenizes the scene well, and significantly improves the stability of the ISRF compared to a classical slit. In Fig. 7a we compare the ISRF shape difference for a 50 % stationary calibration scene for a case with a classical slit and a case with SH. The SH improves the ISRF stability by almost an order of magnitude. ~~On the other hand, comatic aberrations degrade the ISRF stability~~ Considering the applicable Earth scene and including the far-field variations, the SH still provides sufficiently stable ISRF stability with respect to the mission requirements for moderate heterogeneous scenes of Sentinel-5/UVNS. This would not be the case for an instrument employed with a classical slit.

In certain scenarios, Sentinel-5/UVNS will fly over Earth scenes with higher contrasts than specified in the applicable Earth scene. This will be the case when flying over cloud fields, water bodies or city to vegetation transitions. However, these scenes are excluded from the mission requirements in terms of scene homogenization. Although sufficient for the purposes of Sentinel-5/UVNS, the capability of the SH to homogenize the scene is not perfect. This imperfection is particularly prominent when considering the calibration scenes. The imperfections originate from the remaining interference fluctuations in the SH

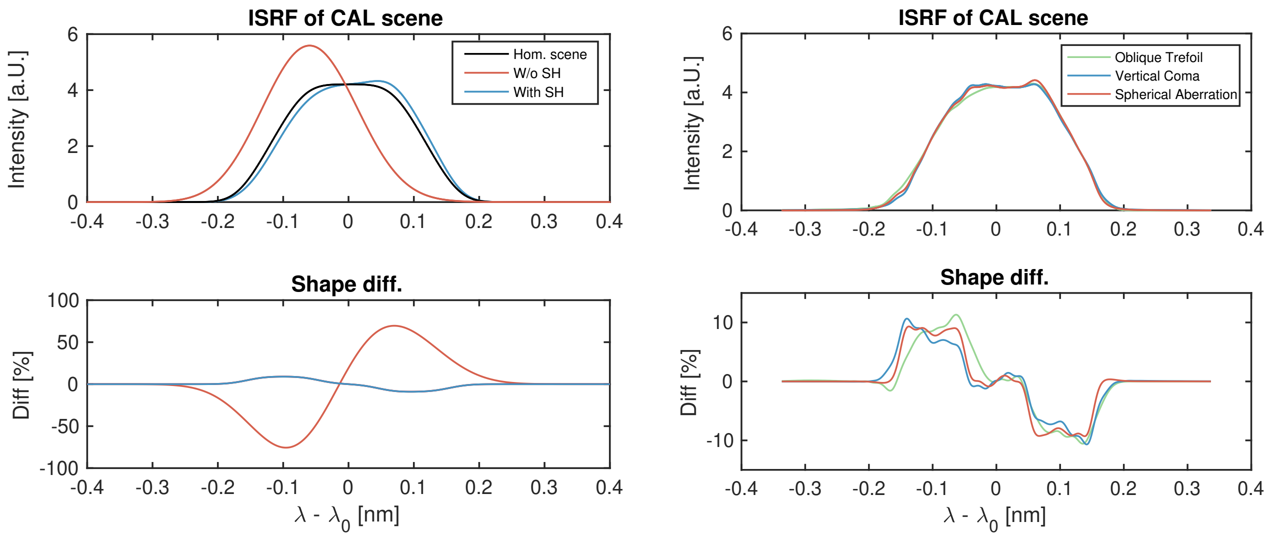

(a) Comparison with classical Slit

(b) ISRF shape difference for exemplarly aberrations

Figure 7. (a) ISRF with and without a slit homogenizer for a heterogeneous 50 % calibration scene. The SH strongly reduces the shape error of the ISRF by an order of magnitude. (b) Comparison between the ISRF shape errors for three exemplary aberrations. The presented aberrations induce a higher maximum shape error but also strongly change the overall shape of the ISRF with respect to the homogeneous reference case.

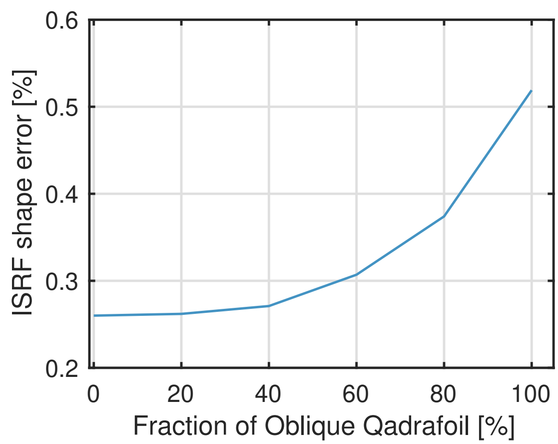

Figure 8. Progression of ISRF shape error from pure oblique quadrafoil aberration to pure defocus aberration. Between the values, we decreased the quadrafoil Zernike coefficient in 20 % steps and at the same time adjusted the defocus coefficient to reach the PSF design size of 6.85 μm again. The plot suggests that the ISRF errors of Zernike combinations are within the ISRF errors of the individual Zernike contributors.

transfer function and are dependent on the wavelength. Higher wavelengths show smaller frequencies and larger peak-to-valley amplitudes of the maxima in ~~terms of shape error and FWHM error. For the S5-ESA-scene, the shape error more than doubles and the FWHM error goes up by a factor of 8. For the calibration scenes, the error contribution gets significantly higher due to higher non uniformity in the spectrograph pupil. As the slit illumination and therefore mixing of the scene contrast in~~ the SH ~~exit plane is the same for all three PSF cases, it seems a valid assumption, that the difference in the relative errors comes only by the non uniform intensity in the spectrograph pupil . As the discrepancy in the values is quite significant, we believe that depending on the mission parameters, this effect should be taken into account for the assessment of the ISRF stability and consequently the performance of the SH. We also conclude, that for the~~ transfer function, which leads to reduced homogenization efficiency. Therefore, the SWIR-3 wavelength channel is the most challenging in terms of scene homogenization.

We observe, that increasing the number of reflections inside the SH will increase the number of stripes in the spectrometer pupil illumination (see Fig. 6c/6d) and reduce the peak to valley amplitude. This would lead to a more homogeneous pupil illumination. More reflection in the SH can be achieved by either increasing the length of the SH or adapting the telescope $F_{\#}$. However, it is advantageous to keep the SH length small to reduce the collimator astigmatism requirements. Note, that a longer SH would not increase the near-field homogenization performance. In addition, more reflections in the SH lead to greater transmission losses at the mirrors. As the errors due to the pupil illumination are small compared to achieved near-field homogenization, it seems favourable to prioritize the first-order design rule given in Caron et al. (2019) and Meister et al. (2017) . The SH shows the best near-field homogenization performance if $F\#_{tel} = l/(2bn)$, where $F\#_{tel}$ is the telescope F-number, l the SH length, b the SH width and n the number of reflections. For Sentinel-5/UVNS~~instrument the impact of this effect is~~, the optimal parameters for SWIR-3 are a telescope $F_{\#}$ of 9.95, a slit length of 9.91 mm and a slit width of 248 μm.

The simulation results of this study still require experimental validation. An initial approach to validate the SH transfer functions was published in Irizar et al. (2019), where they showed good agreement between the simulation and the experimental result for a single SH incidence angle. The verification of the full transfer function including the full FoV range is pending. The SH far-field effects investigated in this study could be determined by measuring the pupil intensity distribution at the grating position by means of an appropriate test bench. The test bench would need to be capable to illuminate the SH entrance plane through a telescope with angles representing the Sentinel-5/UVNS FoV. Further, the astigmatism of ~~second-order and doesn't degrade the performance of~~ the SH ~~significantly~~needs to be compensated which could be done by introducing a cylindrical lens in the collimator system.

Apart from the mirror based SH discussed in this study, future remote sensing instruments investigate the technology of another slit homogenizer technology which is based on rectangular multimode fibre bundles. These devices are based on the same principle as the mirror based SH but enable to homogenize the scene in ACT and ALT direction (Amann et al., 2019) and provide enhanced performance over extreme albedo variations.

Table 1. Applicable Earth scene - ISRF stability. Requirements: Shape error < 2 %, FWHM error < 1 %, Centroid error 0.0125 nm. The presented errors combine the remaining SH exit non-uniformity (near-field) and effects due to the variations of the spectrograph pupil illumination (far-field). The strength of the aberrations are chosen such that the spot size matches the case of a PSF size of 6.85 μm (80 % EE).

OSA/ANSI Index	Zernike Term	Shape Error [%]	FWHM Error [%]	Centroid Error [nm]
3	Oblique astigmatism	0.344	0.056	0.0003
4	Defocus	0.260	0.023	0.0002
5	Vertical astigmatism	0.260	0.023	0.0002
6	Vertical trefoil	0.409	0.020	0.0002
7	Vertical coma	0.388	0.032	0.0003
8	Horizontal coma	0.490	0.055	0.0003
9	Oblique trefoil	0.451	0.103	0.0003
10	Oblique quadrafoil	0.519	0.017	0.0003
11	Oblique second. astigmatism	0.398	0.011	0.0003
12	Primary spherical	0.372	0.040	0.0003
13	Vertical second. astigmatism	0.382	0.040	0.0003
14	Vertical quadrufoil	0.380	0.030	0.0003
Mixture 1 - Defocus (33 %) / V. astig. (33 %) / Prim. sph. (33 %)		0.334	0.017	0.0002
Mixture 2 - O. astig (36 %) / V. coma (32 %) / O.s. astig (32 %)		0.382	0.040	0.0002
With SH - Gaussian PSF		0.248	0.010	0.0003
Classical Slit - Gaussian PSF		2.54	0.061	0.0030

Table 2. 50 % CAL scene - ISRF stability. Remark: ISRF values are exaggerated with respect to real flight scenarios. Calibration scenes are used for on-ground SH performance validation.

OSA/ANSI Index	Zernike Term	Shape Error [%]	FWHM Error [%]	Centroid Error [nm]
3	Oblique astigmatism	8.507	1.589	0.008
4	Defocus	6.883	0.884	0.004
5	Vertical astigmatism	6.883	0.884	0.004
6	Vertical trefoil	9.230	0.833	0.008
7	Vertical coma	9.320	2.025	0.008
8	Horizontal coma	11.549	2.250	0.008
9	Oblique trefoil	11.320	0.566	0.008
10	Oblique quadrafoil	11.859	3.316	0.008
11	Oblique second. astigmatism	10.059	3.750	0.008
12	Primary spherical	10.686	0.382	0.008
13	Vertical second. astigmatism.	11.136	0.465	0.008
14	Vertical quadrufoil	10.127	0.928	0.008
Mixture 1 - Defocus (33 %) / V. astig. (33 %) / Prim. sph. (33 %)		7.367	0.442	0.004
Mixture 2 - O. astig (36 %) / V. coma (32 %) / O.s. astig (32 %)		9.982	0.849	0.008
With SH - Gaussian PSF		6.363	0.566	0.008
Classical Slit - Gaussian PSF		65.664	37.039	0.059

6 Conclusion

~~In this paper we presented an end-to-end simulation of the Sentinel-5/UVNS Slit-homogenizer and demonstrated the impact of non-uniform scenes on the spectrograph pupil intensity distribution. A scenedependency of~~ The presented study continues the investigation by Caron et al. (2019) and Meister et al. (2017) on the mirror based slit homogenizer technology. While the preceding studies were considering the homogenization of the SH exit plane, here, we extend the models by including the electric field propagation through the subsequent spectrograph. The slit homogenizer not only homogenizes the slit illumination, but also modifies the spectrograph illumination dependent on the input scene. The variations in the spectrograph pupil illumination will lead to ~~similar ISRF distortion as due to non-uniform slit illuminations resulting in a pseudo-noise contribution in the measured ToA reflectance. This error~~ a scene dependent weighting of the geometrical aberrations in the optical system, which cause an additional distortion source of the ~~final data product will affect the accuracy of the trace gas derivation of the reflectance spectra. The severity of the error is crucially dependent on contrast, which the instrument will see during a single integration time. A representative scene~~ ISRF. The phenomena is particularly prominent in the presence of extreme on-ground albedo contrasts. This will be the case, when the instrument flies over clouds or water bodies. However, in the context of the Sentinel-5/UVNS instrument~~has a rather weak contrast and therefore the instrument fulfils the ISRF specifications in order to meet the Level-2 performance requirements of the mission. In contrast to this, future missions like CO2M have to be compliant with higher contrast scenes with almost a sharp transition from dark to bright slit illuminations. In such cases,~~ , these scenes are excluded from the mission requirements.

We observe, that the impact of spectrograph pupil illumination variations is small compared to the ~~spectrometer illumination will vary drastically and puts another uncertainty to the ISRF due to PSF variations.We confirmed that Sentinel-5/UVNS meets the requirements on the ISRF knowledge including the modified intensity distribution in the spectrograph pupil and accounting for optical aberrations present in the spectrometer optics. The contribution of the residual errors due to representative inhomogeneous ToA scenes~~ error due to non-uniform slit illumination and the ISRF distortion is primary driven by the remaining near-field variations after the SH. The inhomogeneity remnants arise from the fluctuations of the interference pattern at the SH exit plane. The strength of the variations is increasing with wavelength. Therefore, this study was conducted in the SWIR-3 channel in order to cover the worst case.

We quantify the ISRF in terms of shape error, FWHM error and centroid error at 2312 nm by an end to end propagation through the SH and the subsequent spectrograph optics. With regard to these figures of merits, our simulation results suggest an increase of the errors depending on the specific type of aberrations impinged on the optics. ISRF errors of combined Zernike polynomials are always within the maximum errors of the individual Zernike constituent. Although the SH changes the spectrometer illumination, it still has significant performance advantages in stabilizing the ISRF compared to a classical slit. For an applicable heterogeneous Earth scene, the SH improves the ISRF shape stability by a factor of 5-10. The remaining residual errors are well below the ~~system requirements~~Sentinel-5/UVNS system requirement, which are: shape error ~~<2 %~~2%, the relative FWHM error ~~<1 %~~ $\leq 1\%$ and the centroid error ~~<0.02 (NIR). The application of the slit homogenizer for missions with high contrast scenes (CO2M) will impose strong variations in the spectrograph pupil and will result in large errors in the~~

~~ISRF and hence significantly degrades the accuracy in the retrieval of the atmospheric composition and therefore the mission product.~~ $<$ 0.0125 nm (SWIR-3).

Data availability. The datasets generated and/or analyzed for this work are available from the corresponding author on reasonable request, subject to confirmation of Airbus Defence and Space GmbH.

Author contributions. Timon Hummel was responsible for the modelling and the analysis of the simulation data supported by all co-authors. Timon Hummel developed the end-to-end model and the approach to quantify the impact on the ISRF supported and revised by Christian Meister. Timon Hummel prepared the manuscript with contributions and critical revision from all co-authors.

Competing interests. The authors declare, that they have no conflict of interest.

Acknowledgements. We thank Corneli Keim, Tobias Lamour, Jess Köhler and Markus Melf (all Airbus Defence and Space) for the helpful comments on a previous version of the manuscript.

References

Amann, S., Duong-Ederer, Q., Haist, T., Sierk, B., Guldimann, B., and Osten, W.: Characterization of fiber-based slit homogenizer devices in the NIR and SWIR, in: International Conference on Space Optics — ICSO 2018, edited by Sodnik, Z., Karafolas, N., and Cugny, B., vol. 11180, pp. 2276 – 2286, International Society for Optics and Photonics, SPIE, https://doi.org/10.1117/12.2536147, https://doi.org/10.1117/12.2536147, 2019.

Berlich, R. and Harnisch, B.: Radiometric assessment method for diffraction effects in hyperspectral imagers applied to the earth explorer 8 mission candidate flex, in: International Conference on Space Optics — ICSO 2014, edited by Sodnik, Z., Cugny, B., and Karafolas, N., vol. 10563, pp. 1475 – 1483, International Society for Optics and Photonics, SPIE, https://doi.org/10.1117/12.2304079, https://doi.org/10.1117/12.2304079, 2017.

Bovensmann, H., Burrows, J. P., Buchwitz, M., Frerick, J., Noël, S., Rozanov, V. V., Chance, K. V., and Goede, A. P. H.: SCIAMACHY: Mission Objectives and Measurement Modes, Journal of the Atmospheric Sciences, 56, 127–150, https://doi.org/10.1175/1520-0469(1999)056<0127:SMOAMM>2.0.CO;2, https://doi.org/10.1175/1520-0469(1999)056<0127:SMOAMM>2.0.CO;2, 1999.

Burrows, J., Hölzle, E., Goede, A., Visser, H., and Fricke, W.: SCIAMACHY—scanning imaging absorption spectrometer for atmospheric chartography, Acta Astronautica, 35, 445 – 451, https://doi.org/https://doi.org/10.1016/0094-5765(94)00278-T, http://www.sciencedirect.com/science/article/pii/009457659400278T, earth Observation, 1995.

Burrows, J. P., Weber, M., Buchwitz, M., Rozanov, V., Ladstätter-Weißenmayer, A., Richter, A., DeBeek, R., Hoogen, R., Bramstedt, K., Eichmann, K.-U., Eisinger, M., and Perner, D.: The Global Ozone Monitoring Experiment (GOME): Mission Concept and First Scientific Results, Journal of the Atmospheric Sciences, 56, 151–175, https://doi.org/10.1175/1520-0469(1999)056<0151:TGOMEG>2.0.CO;2, https://doi.org/10.1175/1520-0469(1999)056<0151:TGOMEG>2.0.CO;2, 1999.

Caron, J., Sierk, B., Bezy, J.-L., Loescher, A., and Meijer, Y.: The CarbonSat candidate mission: radiometric and spectral performances over spatially heterogeneous scenes, in: International Conference on Space Optics — ICSO 2014, edited by Sodnik, Z., Cugny, B., and Karafolas, N., vol. 10563, pp. 1019 – 1027, International Society for Optics and Photonics, SPIE, https://doi.org/10.1117/12.2304186, https://doi.org/10.1117/12.2304186, 2017.

Caron, J., Kruizinga, B., and Vink, R.: Slit homogenizers for Earth observation spectrometers: overview on performance, present and future designs, in: International Conference on Space Optics — ICSO 2018, edited by Sodnik, Z., Karafolas, N., and Cugny, B., vol. 11180, pp. 402 – 417, International Society for Optics and Photonics, SPIE, https://doi.org/10.1117/12.2535957, https://doi.org/10.1117/12.2535957, 2019.

EOP PIO, E.: Sentinel-5 UVNS Phase A/B1 Reference Spectra, 2011.

Gerilowski, K., A, T., T, K., Buchwitz, M., Bertagnolio, P., F, B., J, E., Burrows, J., and H, B.: MAMAP - A new spectrometer system for column-averaged methane and carbon dioxide observations from aircraft: Instrument description and performance analysis, Atmospheric Measurement Techniques, 4, https://doi.org/10.5194/amt-4-215-2011, 2011.

Goodman, J. W.: Introduction to Fourier optics, vol. 1, 2005.

Hu, H., Hasekamp, O., Butz, A., Galli, A., Landgraf, J., Aan de Brugh, J., Borsdorff, T., Scheepmaker, R., and Aben, I.: The operational methane retrieval algorithm for TROPOMI, Atmospheric Measurement Techniques, 9, 5423–5440, https://doi.org/10.5194/amt-9-5423-2016, https://amt.copernicus.org/articles/9/5423/2016/, 2016.

Irizar, J., Melf, M., Bartsch, P., Koehler, J., Weiss, S., Greinacher, R., Erdmann, M., Kirschner, V., Albinana, A. P., and Martin, D.: Sentinel-5/UVNS, in: International Conference on Space Optics — ICSO 2018, edited by Sodnik, Z., Karafolas, N., and Cugny, B., vol. 11180, pp.

41 – 58, International Society for Optics and Photonics, SPIE, https://doi.org/10.1117/12.2535923, https://doi.org/10.1117/12.2535923, 2019.

Landgraf, J., aan de Brugh, J., Scheepmaker, R., Borsdorff, T., Hu, H., Houweling, S., Butz, A., Aben, I., and Hasekamp, O.: Carbon monoxide total column retrievals from TROPOMI shortwave infrared measurements, Atmospheric Measurement Techniques, 9, 4955–4975, https://doi.org/10.5194/amt-9-4955-2016, https://amt.copernicus.org/articles/9/4955/2016/, 2016.

Meister, C., Bauer, M., Keim, C., and Irizar, J.: Sentinel-5/UVNS instrument: the principle ability of a slit homogenizer to reduce scene contrast for earth observation spectrometer, in: SPIE Proceedings Vol.10423, Sensors, Systems, and Next-Generation Satellites XXI; 104231E, https://doi.org/10.1117/12.2278619, 2017.

Noël, S., Bramstedt, K., Bovensmann, H., Gerilowski, K., Burrows, J. P., Standfuss, C., Dufour, E., and Veihelmann, B.: Quantification and mitigation of the impact of scene inhomogeneity on Sentinel-4 UVN UV-VIS retrievals, Atmospheric Measurement Techniques, 5, 1319–1331, https://doi.org/10.5194/amt-5-1319-2012, https://amt.copernicus.org/articles/5/1319/2012/, 2012.

Sierk, B., Bezy, J.-L., Loescher, A., and Meijer, Y.: The European CO2 Monitoring Mission: observing anthropogenic greenhouse gas emissions from space, in: International Conference on Space Optics — ICSO 2018, edited by Sodnik, Z., Karafolas, N., and Cugny, B., vol. 11180, pp. 237 – 250, International Society for Optics and Photonics, SPIE, https://doi.org/10.1117/12.2535941, https://doi.org/10.1117/12.2535941, 2019.

Thibos, L. N., Applegate, R. A., Schwiegerling, J. T., and and, R. W.: Standards for Reporting the Optical Aberrations of Eyes, in: Vision Science and its Applications, p. SuC1, Optical Society of America, https://doi.org/10.1364/VSIA.2000.SuC1, http://www.osapublishing.org/abstract.cfm?URI=VSIA-2000-SuC1, 2000.

Veefkind, J., Aben, I., McMullan, K., Förster, H., de Vries, J., Otter, G., Claas, J., Eskes, H., de Haan, J., Kleipool, Q., van Weele, M., Hasekamp, O., Hoogeveen, R., Landgraf, J., Snel, R., Tol, P., Ingmann, P., Voors, R., Kruizinga, B., Vink, R., Visser, H., and Levelt, P.: TROPOMI on the ESA Sentinel-5 Precursor: A GMES mission for global observations of the atmospheric composition for climate, air quality and ozone layer applications, Remote Sensing of Environment, 120, 70–83, https://doi.org/https://doi.org/10.1016/j.rse.2011.09.027, https://www.sciencedirect.com/science/article/pii/S0034425712000661, the Sentinel Missions - New Opportunities for Science, 2012.

Voors, R., Dobber, M., Dirksen, R., and Levelt, P.: Method of calibration to correct for cloud-induced wavelength shifts in the Aura satellite's Ozone Monitoring Instrument, Appl. Opt., 45, 3652–3658, https://doi.org/10.1364/AO.45.003652, http://ao.osa.org/abstract.cfm?URI=ao-45-15-3652, 2006.